just below the bifurcation of the deep femoral artery.

ACKNOWLEDGMENTS

The authors wish to thank Ms. Y Shinozaki for technical assistance. This work was supported by Grants-in-Aid for Scientific Research (15390066, 15659285, 16790761) from the MECSST; The Science Frontier Program of MECSST; Industrial Technology Research Grant Program in '03 from NEDO of Japan; The Research Grants for Cardiovascular Disease (H16C-6), Health and Labour Sciences Research Grants (nano-001, genome-005 and Saisei-003) from the MHLW; the Promotion Fundamental Studies in Health Science of the OPSR, Japan; Tokyo University of Agriculture Soken-Project Research Aid.

REFERENCES

1) Skjeldal S, Grogaard B, Reikeras O, Muller C, Torvik A, and Svindland A. Model for skeletal muscle ischemia in rat hindlimb: evaluation of reperfusion and necrosis. Eur Surg Res 1991; 23: 355-365.
2) Kalka C, Masuda H, Takahashi T, Kalka-Moll WM, Silver M, Kearney M, *et al*: Transplantation of ex vivo expanded endothelial progenitor cells for therapeutic neovascularization. Proc Natl Acad Sci U S A 2000; 97: 3422-3427.
3) Iwaguro H, Yamaguchi J, Kalka C, Murasawa S, Masuda H, Hayashi S, *et al*: Endothelial progenitor cell vascular endothelial growth factor gene transfer for vascular regeneration. Circulation 2002; 105: 732-738.
4) Milia AF, Salis MB, Stacca T, Pinna A, Madeddu P, Trevisani M, *et al*: Protease-activated receptor-2 stimulates angiogenesis and accelerates hemodynamic recovery in a mouse model of hindlimb ischemia. Circ Res 2002; 91: 346-352.
5) Chatterjee BD and Chakraborti CK: Ischaemic mouse thigh model for evaluation of pathogenicity of non- clostridial anaerobes. Indian J Med Res 1989; 89: 36-39.
6) Murohara T, Asahara T, Silver M, Bauters C, Masuda H, Kalka C, *et al*: Nitric oxide synthase modulates angiogenesis in response to tissue ischemia. J Clin Invest 1998;101: 2567-2578.
7) Kanno S, Oda N, Abe M, Saito S, Hori K, Handa Y, *et al*: Establishment of a simple and practical procedure applicable to therapeutic angiogenesis. Circulation 1999; 99: 2682-2687.
8) Rivard A, Silver M, Chen D, Kearney M, Magner M, Annex B, *et al*: Rescue of diabetes-related impairment of angiogenesis by intramuscular gene therapy with adeno-VEGF. Am J Pathol 1999; 154: 355-363.
9) Byun J, Heard JM, Huh JE, Park SJ, Jung EA, Jeong JO, *et al*: Efficient expression of the vascular endothelial growth factor gene in vitro and in vivo, using an adeno-associated virus vector. J Mol Cell Cardiol 2001; 33: 295-305.
10) Wiersema AM, Oyen WJ, Dirksen R, Verhofstad AA, Corstens FH, and van der Vliet JA: Early assessment of skeletal muscle damage after ischaemia-reperfusion injury using Tc-99m-glucarate. Cardiovasc Surg 2000: 186-191.
11) Messina LM, Brevetti LS, Chang DS, Paek R, and Sarkar R: Therapeutic angiogenesis for critical limb ischemia: invited commentary. J Control Release 2002; 78: 285-294.
12) Kuwabara E, Furuyama F, Ito K, Tanaka E, Hattan N, Fujikura H, *et al*: Inhomogeneous vasodilatory responses of rat tail arteries to heat stress: evaluation by synchrotron radiation microangiography. Jpn J Physiol 2002; 52: 403-408.
13) Kasahara H, Tanaka E, Fukuyama N, Sato E, Sakamoto H, Tabata Y, *et al*: Biodegradable gelatin hydrogel potentiates the angiogenic effect of fibroblast growth factor 4 plasmid in rabbit hindlimb ischemia. J Am Coll Cardiol 2003; 41: 1056-1062.

Journal of the American College of Cardiology
© 2006 by the American College of Cardiology Foundation
Published by Elsevier Inc.

Vol. 48, No. 1, 2006
ISSN 0735-1097/06/$32.00
doi:10.1016/j.jacc.2006.04.008

PRECLINICAL STUDY

Erythropoietin Enhances Neovascularization of Ischemic Myocardium and Improves Left Ventricular Dysfunction After Myocardial Infarction in Dogs

Akio Hirata, MD,* Tetsuo Minamino, MD, PHD,* Hiroshi Asanuma, MD, PHD,* Masashi Fujita, MD,* Masakatsu Wakeno, MD,† Masafumi Myoishi, MD,† Osamu Tsukamoto, MD,* Ken-ichiro Okada, MD,* Hidekazu Koyama, BS,* Kazuo Komamura, MD, PHD,§ Seiji Takashima, MD, PHD,* Yoshiro Shinozaki, MD,‖ Hidezo Mori, MD, PHD,§ Masamichi Shiraga, MD, PHD,‡ Masafumi Kitakaze, MD, PHD, FACC,§ Masatsugu Hori, MD, PHD, FACC*

Osaka and Kanagawa, Japan

OBJECTIVES We investigated the effects of erythropoietin (EPO) on neovascularization and cardiac function after myocardial infarction (MI).

BACKGROUND Erythropoietin exerts antiapoptotic effects and mobilizes endothelial progenitor cells (EPCs).

METHODS We intravenously administered EPO (1,000 IU/kg) immediately [EPO(0) group], 6 h [EPO(6h) group], or 1 week [EPO(1wk) group] after the permanent ligation of the coronary artery in dogs. Control animals received saline immediately after the ligation.

RESULTS The infarct size 6 h after MI was significantly smaller in the EPO(0) group than in the control group (61.5 ± 6.0% vs. 22.9 ± 2.2%). One week after MI, the circulating CD34-positive mononuclear cell numbers in both the EPO(0) and the EPO(6h) groups were significantly higher than in the control group. In the ischemic region, the capillary density and myocardial blood flow 4 weeks after MI was significantly higher in both the EPO(0) and the EPO(6h) groups than in the control group. Four weeks after MI, left ventricular (LV) ejection fraction in the EPO(6h) (48.6 ± 1.9%) group was significantly higher than that in either the control (41.9 ± 0.9%) or the EPO(1wk) (42.6 ± 1.2%) group but significantly lower than that in the EPO(0) group (56.1 ± 2.3%). The LV end-diastolic pressure 4 weeks after MI in both the EPO(0) and the EPO(6h) groups was significantly lower than either the control or the EPO(1wk) group. Hematologic parameters did not differ among the groups.

CONCLUSIONS In addition to its acute infarct size-limiting effect, EPO enhances neovascularization, likely via EPC mobilization, and improves cardiac dysfunction in the chronic phase, although it has time-window limitations. (J Am Coll Cardiol 2006;48:176–84) © 2006 by the American College of Cardiology Foundation

Erythropoietin (EPO) is a cytokine that promotes proliferation and differentiation of erythroid precursor cells (1) and is widely used for the treatment of anemia in patients with chronic renal failure (2). Erythropoietin can also exert antiapoptotic and radical scavenger effects on nonerythroid cells (3,4). Indeed, we and others showed that an administration of EPO before or shortly after the onset of ischemia

See page 185

reduced myocardial infarct size and improved cardiac function in acute phases (5–8). Another interesting nonerythroid function of EPO is the promotion of endothelial progenitor cell (EPC) mobilization in animals and humans (9–11), which may enhance neovascularization of ischemic areas (12,13). We hypothesized that EPO increases blood supply to ischemic regions through promoting neovascularization and improves cardiac dysfunction after ischemic insult. Thus, the goal of this study was to characterize the effects of EPO on neovascularization and cardiac function after myocardial infarction (MI) in the chronic phase.

METHODS

All procedures were performed in conformity with the Guide for the Care and Use of Laboratory Animals (NIH publication no. 85-23, 1996 revision) and were approved by the Osaka University Committee for Laboratory Animal Use.

Instrumentation. Forty-seven beagle dogs (Kitayama Labes, Yoshiki Farm Gifu, Japan), weighing 8 to 12 kg were used in these experiments. After an intravenous injection of sodium pentobarbital (15 mg/kg), the dogs were intubated and ventilated. General anesthesia was maintained with 0.5% to 2.0% inhaled isoflurane. After baseline echocardiography and hemodynamic assessment, minimal thoracot-

From the Departments of *Cardiovascular Medicine, †Bioregulatory Medicine, and ‡Hematology and Oncology, Osaka University Graduate School of Medicine, Suita, Osaka, Japan; §Cardiovascular Division of Internal Medicine, National Cardiovascular Center, Suita, Osaka, Japan; and the ‖Department of Physiological Science, Tokai University School of Medicine, Isehara, Kanagawa, Japan.

Manuscript received June 14, 2005; revised manuscript received November 10, 2005, accepted November 30, 2005.

Abbreviations and Acronyms

ABP	= arterial mean blood pressure
Dil-ac-LDL	= 1,1′-dioctadecyl-3,3,3′,3′-tetramethylindocarbocyanine-labeled acetylated low density lipoprotein
EPC	= endothelial progenitor cell
EPO	= erythropoietin
HR	= heart rate
LAD	= left anterior descending coronary artery
LCX	= left circumflex coronary artery
LV	= left ventricle/ventricular
LVEDD	= left ventricular end-diastolic dimension
LVEDP	= left ventricular end-diastolic pressure
MBF	= myocardial blood flow
MI	= myocardial infarction
MNC	= mononuclear cell
UEA-I	= *Ulex europaeus* agglutinin I
VEGF	= vascular endothelial growth factor

omy was performed, and then the left anterior descending coronary artery (LAD) was ligated just distal to the first diagonal branch. To ensure that all animals included in the data analysis were exposed to a similar extent of ischemia, animals with excessive myocardial collateral blood flow (>15 ml/100 g/min) were excluded from study as previously described (14).

Experimental protocols. ACUTE EFFECTS OF EPO ON MYOCARDIAL INFARCT SIZE. Either a single dose of EPO (1,000 IU/kg; 5 ml) (n = 6) or the same volume of saline (n = 6) was administered intravenously immediately after the LAD ligation. Regional myocardial blood flow (MBF), area at risk, and infarct size at 6 h after the LAD ligation were determined as described previously (Fig. 1) (14). Recombinant human EPO was provided by Chugai Pharmaceutical Co. Ltd. (Tokyo, Japan). Recombinant human EPO is effective for correcting anemia in the beagle dog (15).

EFFECTS OF IMMEDIATE OR DELAYED TREATMENT WITH EPO ON NEOVASCULARIZATION AND CARDIAC FUNCTION. A single dose of EPO (1,000 IU/kg; 5 ml) was administered intravenously immediately [EPO(0) group, n = 8], 6 h [EPO(6h) group, n = 8], or 1 week [EPO(1wk) group, n = 7] after the LAD ligation. Control animals received the same volume of saline (control group, n = 8) immediately after the LAD ligation.

Hematologic parameters. Blood was sampled from a peripheral vein under pentobarbital (15 mg/kg) anesthesia at the time points indicated in Figure 2. Hematologic parameters, including hematocrit, white blood cell count, and platelet count, were measured.

Cytokine measurements. Plasma levels of vascular endothelial growth factor (VEGF) were measured by enzyme-linked immunosorbent assay (R & D Systems, Minneapolis, Minnesota). The detection limit of the assays was 9 pg/ml. The reliability of this assay in dogs has already been reported previously (16).

Quantification of CD34-positive mononuclear cells. The circulating CD34-positive mononuclear cells (CD34+MNCs) were quantified at the time points indicated in Figure 2. In brief, peripheral white blood cells were stained with a phycoerythrin-conjugated anticanine CD34 monoclonal antibody (BD Pharmingen, San Diego, California). Samples were then subjected to a two-dimensional side-scatter-fluorescence dot plot analysis (FACScan, Becton-Dickinson, Tokyo, Japan). After appropriate gating of

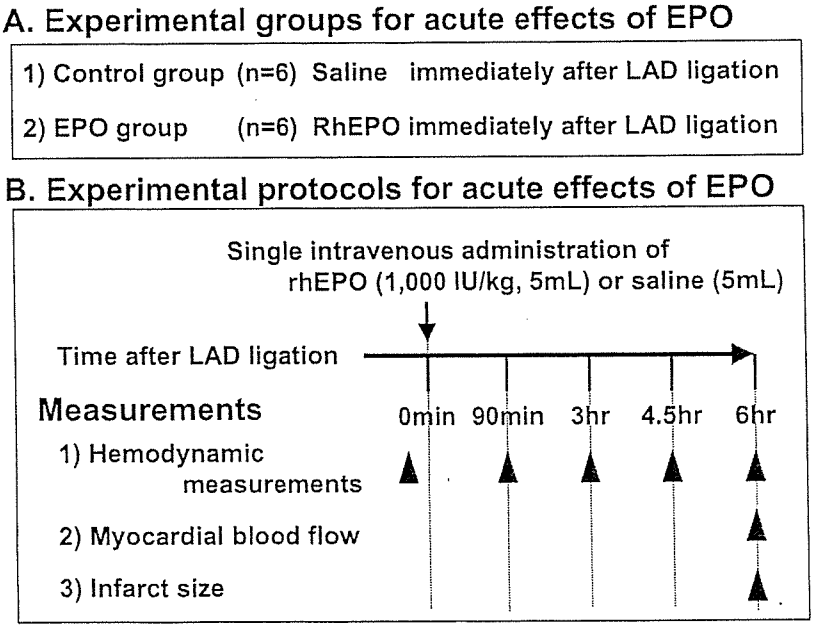

Figure 1. Experimental protocols to investigate acute effects of erythropoietin (EPO) on myocardial infarct size. LAD = left anterior descending coronary artery; RhEPO = recombinant human erythropoietin.

JACC Vol. 48, No. 1, 2006
July 4, 2006:176–84

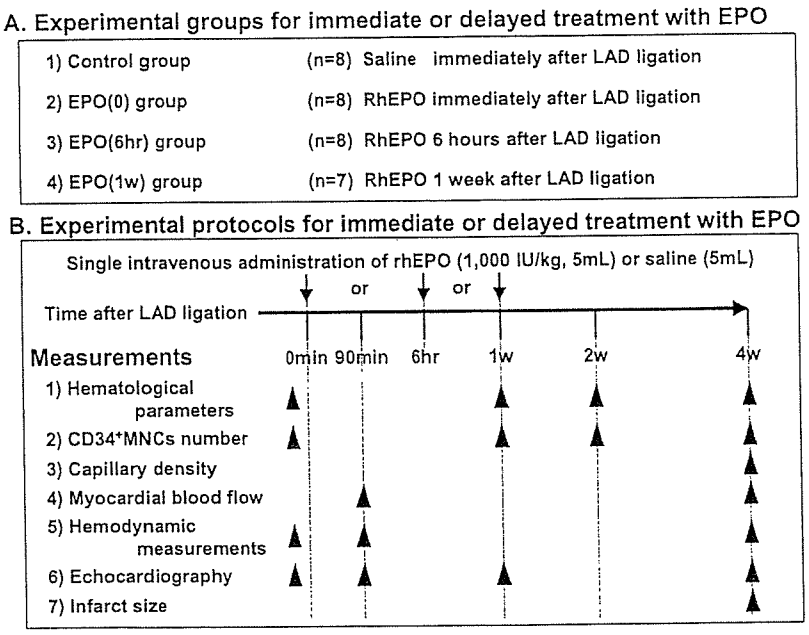

Figure 2. Experimental protocols to investigate effects of immediate or delayed treatment with erythropoietin (EPO) on neovascularization and cardiac function. CD34+MNC = CD34-positive mononuclear cell; other abbreviations as in Figure 1.

MNCs, the number of CD34+MNCs with low cytoplasmic granularity (low sideward scatter) was quantified and expressed as the number of cells per 1-μl blood sample.

In vitro MNC culture assay. Circulating MNCs were isolated from blood (10 ml) of dogs at baseline and 1 week after MI in the control and EPO(0) groups (n = 4 each) by Ficoll density-gradient centrifugation. After MNCs (107 per well) were plated in Medium 199 (Gibco, Grand Island, New York) supplemented with 20% fetal calf serum and antibiotics on human fibronectin-coated six-well dishes. After 7 days in culture, adherent cells were stained for the uptake of 1,1′-dioctadecyl-3,3,3′,3′-tetramethylindocarbocyanine-labeled acetylated low-density lipoprotein (DiI-ac-LDL) (Biomedical Technologies, Stoughton, Massachusetts) and the binding of fluorescein isothiocyanate-labeled *Ulex europaeus* agglutinin I (UEA-I) (Vector Laboratories, Peterborough, England). Double-staining cells were quantified by examining five random microscopic fields (×200 power) (10,11).

Histologic assessments. Four weeks after MI, myocardial tissue was sampled from both ischemic (LAD) and nonischemic (left circumflex coronary artery [LCX]) regions in each group. The tissues in the ischemic region were identified as the edge of the region showing necrosis. These samples were then fixed in 10% buffered formalin, embedded in paraffin, and serially sectioned in the frontal plane at 5-μm thickness. Endothelial cells were immunohistologically stained using rabbit antihuman von Willebrand factor antibody (Dako, Kyoto, Japan) and the Envision+/HRP Kit (Dako) (17). The peroxidase was visualized by incubation with 3,3'-diaminobenzidine, followed by incubation with a DAB-enhancing solution (Dako). We counted the numbers of capillaries and cardiomyocytes in 20 random high-power fields (×400 power), and then calculated the average capillary density and capillary-to-myocyte ratio (18).

Measurements of regional MBF. Regional MBF was determined as described previously (19). Nonradioactive microspheres (Sekisui Plastic Co., Tokyo, Japan) made of inert plastic were labeled with bromine or niobium. Microspheres were administered at 90 min and 4 weeks after MI. The MBF in the LAD region was calculated according to the following formula: time flow = (tissue count) × (reference flow)/(reference count), and was expressed in ml/g wet weight/min.

Hemodynamic measurements. Hemodynamic parameters, such as arterial mean blood pressure (ABP), heart rate (HR), and left ventricular end-diastolic pressure (LVEDP), were measured at the time points indicated in Figure 2. A 5-F sidearm sheath (Radifocus, Terumo, Tokyo, Japan) was placed in the right femoral artery for hemodynamic measurements. A 4-F pigtail catheter (Outlook, Terumo) was placed in the LV for measurement of LVEDP and was connected to a pressure transducer (model DX-200, Nihon Kohden, Tokyo, Japan). The ABP and HR were monitored via the 5-F sidearm sheath.

Echocardiography. Cardiac function was assessed by echocardiography (Sonos 5500, S4-probe, 2-4 MHz, Philips, Bothell, Washington) at the time points indicated in Figure 2. Short-axis views were recorded at the level of midpapillary muscles, and two-dimensional and M-mode views were recorded at the same level. Measurements of left ventricular end-diastolic dimension (LVEDD) and LV ejection fraction were obtained from M-mode views. All measurements were made by one observer, who was blinded with respect to the identity of the tracings.

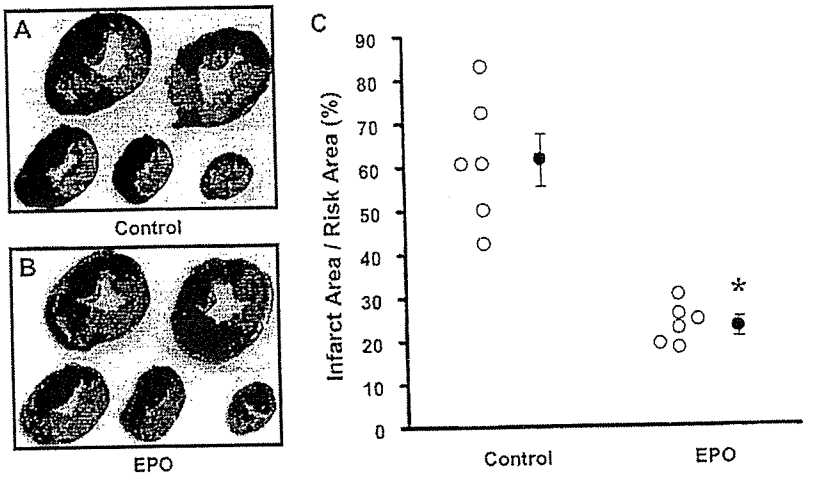

Figure 3. Representative left ventricular cross sections at 6 h after myocardial infarction (MI) in dogs with (B) and without (A) erythropoietin (EPO) treatment. (C) Infarct size at 6 h after MI. *p < 0.05 vs. the control group. **Open circles** = infarct size in each animal.

Infarct size 4 weeks after MI. Myocardial infarct area was determined at the end of the protocol by triphenyltetrazolium chloride staining as described previously (14). Infarct size was expressed as a percentage of the total LV area.

Statistical analysis. Results are expressed as the mean ± standard error of the mean. Comparisons of the time course of the change between groups were performed using two-way repeated measures analysis of variance. Comparisons of other data between groups were performed using one-way factional analysis of variance. If statistical significance was found for a group, a time effect, or a group-by-time interaction, further comparisons were made with paired *t* tests between all possible pairs of four groups at individual time points. The Bonferroni-Holm procedure was used for correction of multiple comparisons. A p value <0.05 was considered to represent statistical significance (20).

RESULTS

Exclusion. Four dogs [acute effects protocol; control: 1, EPO: 0, delayed treatment effects protocol; control: 1, EPO(0): 1, EPO(6h): 0, EPO(1wk): 1] were excluded from analysis because of excessive regional MBF (>15 ml/100 g/min). Thus, 12 and 31 dogs in acute and delayed EPO treatment protocols, respectively, were included.

Acute effects of EPO on infarct size. Myocardial infarct size was significantly smaller in animals receiving EPO compared with those that received saline, but there was no significant difference in regional MBF (9.0 ± 1.0 ml/100 g/min vs. 8.5 ± 1.2 ml/100 g/min) or area at risk (42.9 ± 2.3% vs. 42.3 ± 0.9%) when comparing the two groups (Fig. 3).

Effects of EPO on hematologic parameters. The average change in hematologic parameters was not different when comparing the three EPO-treated groups and the control group over the 4-week experimental protocol (Table 1).

Plasma VEGF levels. Table 2 shows the time course of changes in plasma VEGF level after MI. The plasma VEGF level was significantly and comparably elevated in both control and EPO(0) groups, peaking on 6 h after MI, and returned to baseline at 1 week after MI.

Circulating CD34+MNCs and in vitro cultured MNCs. Figure 4A shows the time course of changes in circulating CD34+MNC number in the different groups. One week after MI, the number of circulating CD34+MNCs increased in all groups. Furthermore, the number of circulating CD34+MNCs at 1 week after MI was higher in the EPO(0) and EPO(6h) groups than in either control or EPO(1wk) group. Two weeks after MI, the number of CD34+MNCs in the control group returned to the baseline. By contrast, the number of CD34+MNCs in the EPO(0) and EPO(6h) groups also decreased but still remained higher than those in either the control or

Table 1. Time Course of Changes in Hematologic Parameters

Parameters	Baseline	1 Week	2 Weeks	4 Weeks
Hematocrit (%)				
Control	52.9 ± 1.7	47.0 ± 1.6	48.9 ± 2.3	53.1 ± 1.8
EPO(0)	52.4 ± 1.1	48.2 ± 1.2	47.9 ± 1.4	53.4 ± 0.7
EPO(6h)	51.5 ± 1.6	49.3 ± 1.6	51.4 ± 1.1	51.3 ± 2.3
EPO(1wk)	48.9 ± 1.0	46.4 ± 1.1	49.4 ± 0.5	50.1 ± 1.0
WBC ($10^3/\mu l$)				
Control	13.8 ± 0.4	15.4 ± 1.4	15.3 ± 0.9	13.5 ± 0.9
EPO(0)	12.6 ± 0.6	14.0 ± 1.1	14.4 ± 0.3	12.3 ± 1.4
EPO(6h)	12.6 ± 0.8	15.6 ± 1.1	13.9 ± 1.0	12.0 ± 0.8
EPO(1wk)	13.1 ± 0.8	14.8 ± 1.2	13.3 ± 0.4	12.9 ± 0.8
Platelet ($10^4/mm^3$)				
Control	27.3 ± 2.0	26.5 ± 1.9	28.4 ± 1.2	26.2 ± 2.0
EPO(0)	28.5 ± 2.0	26.8 ± 4.3	27.0 ± 3.4	28.2 ± 1.8
EPO(6h)	26.9 ± 0.9	27.0 ± 1.4	26.1 ± 1.8	26.1 ± 1.5

Data are presented as mean ± SEM (n = 7 to 8).
EPO = erythropoietin; WBC = white blood cell.

Table 2. Time Course of Changes in Plasma VEGF Levels

Groups	n	Baseline	6 Hours	1 Week	2 Weeks
VEGF (pg/ml)					
Control	4	<9.0	22.5 ± 3.3*	<9.0	<9.0
EPO(0)	4	<9.0	21.6 ± 5.0*	<9.0	<9.0

Data are presented as mean ± SEM. *p < 0.05 vs. baseline.
EPO = erythropoietin; VEGF = vascular endothelial growth factor.

JACC Vol. 48, No. 1, 2006
July 4, 2006:176–84

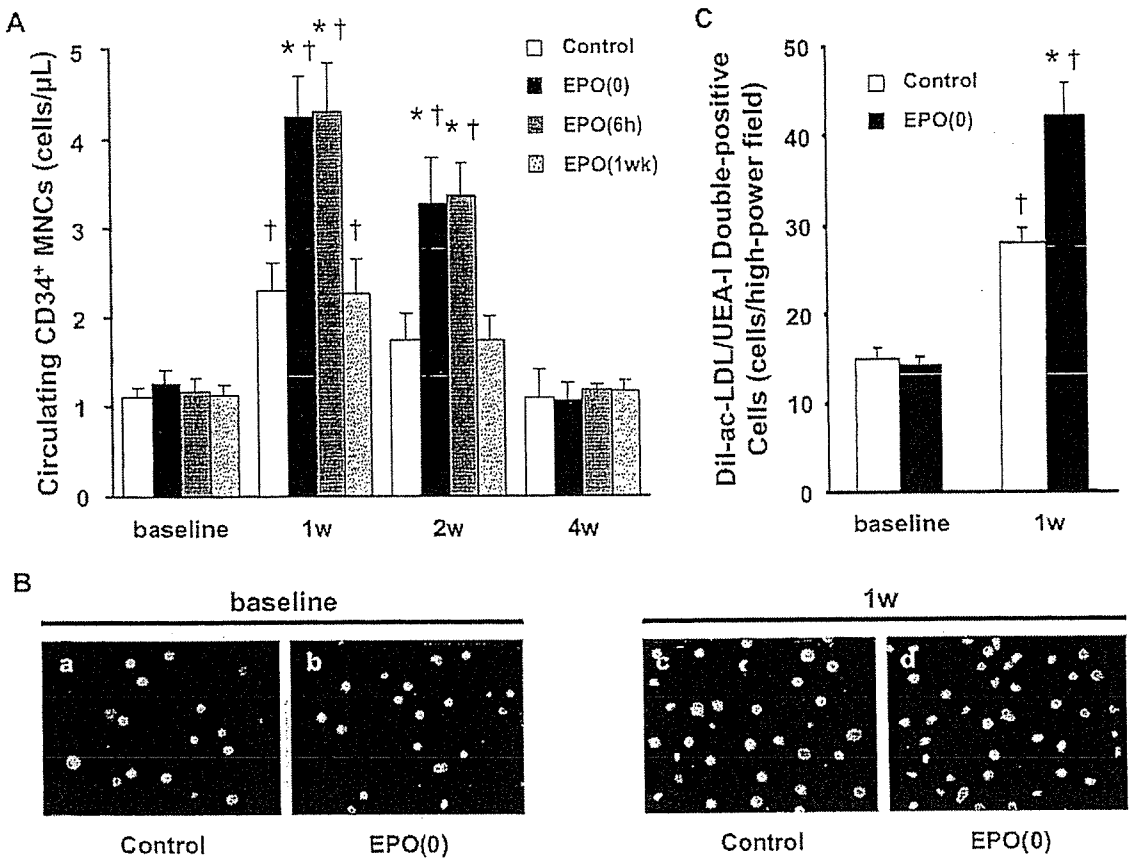

Figure 4. (A) Time course of changes in circulating CD34+MNC count after left anterior descending coronary artery (LAD) ligation in different experimental groups. (B) Representative images of double-stained cultured cells (1,1′-dioctadecyl-3,3,3′,3′-tetramethylindocarbocyanine-labeled acetylated low density lipoprotein [Dil-ac-LDL] and *Ulex europaeus* agglutinin I [UEA-I]) at baseline (a, b) and 1 week after LAD ligation (c, d) from dogs with and without erythropoietin (EPO) treatment immediately after LAD ligation. (C) Quantitative analysis of endothelial progenitor cell culture assay. *$p <$ 0.05 vs. the control group. †$p < 0.05$ vs. baseline.

EPO(1wk) group. Furthermore, the administration of EPO 1 week after the LAD ligation did not affect the number of CD34+MNCs at any given time point.

In the culture assay of MNCs, the number of Dil-ac-LDL/UEA-I double-positive cells obtained from blood 1 week after MI increased compared with that at baseline in both control and EPO(0) groups. Importantly, the double-positive cell number obtained from blood 1 week after MI in the EPO(0) group was significantly higher than in the control group (Figs. 4B and 4C).

Capillary density and regional MBF. Figure 5A shows the representative immunohistologic findings in the non-ischemic (panels a to d) and ischemic (panels e to h) regions at 4 weeks after MI. In the nonischemic region, there was no difference in the capillary density and capillary-to-myocyte ratio when comparing groups. In the ischemic region, the capillary-to-myocyte ratio as well as capillary density was significantly higher in the EPO(0) and EPO(6h) groups, but not in the EPO(1wk) group, than in the control group (Figs. 5B to 5C).

Figure 6 shows the changes in regional MBF in the ischemic regions in different experimental groups. There was no significant difference in MBF at 90 min when comparing experimental groups. At 4 weeks after MI, MBF was more increased in the EPO(0) and EPO(6h) groups, but not in the EPO(1wk) group, than in the control group.

Effects of immediate or delayed EPO treatment on cardiac function and infarct size. Throughout the experimental protocols, there was no difference in either ABP or HR when comparing the groups (Table 3).

Figure 7 shows the time course of changes in LVEF (panel A), LVEDD (panel B), and LVEDP (panel C) in different experimental groups. There were no significant differences in baseline LVEF, LVEDD, and LVEDP when comparing the groups.

Ninety minutes, 1 week, and 4 weeks after MI, LVEF was higher in the EPO(0) group than in the other groups. Ninety minutes and 1 week after MI, there was no difference in LVEF when comparing the EPO(6h) group and the control group. When comparing the time points of 1 week and 4 weeks after MI, LVEF decreased in the control and the EPO(1wk) groups but not in the EPO(6h) group. One and 4 weeks after MI, LVEDD was lower in the EPO(0) group than in the other groups. When comparing the time points of 1 week and 4 weeks after MI, LVEDD increased in the control and EPO(1wk) groups but not in the EPO(6h) group. Ninety minutes after MI, LVEDP was lower in the

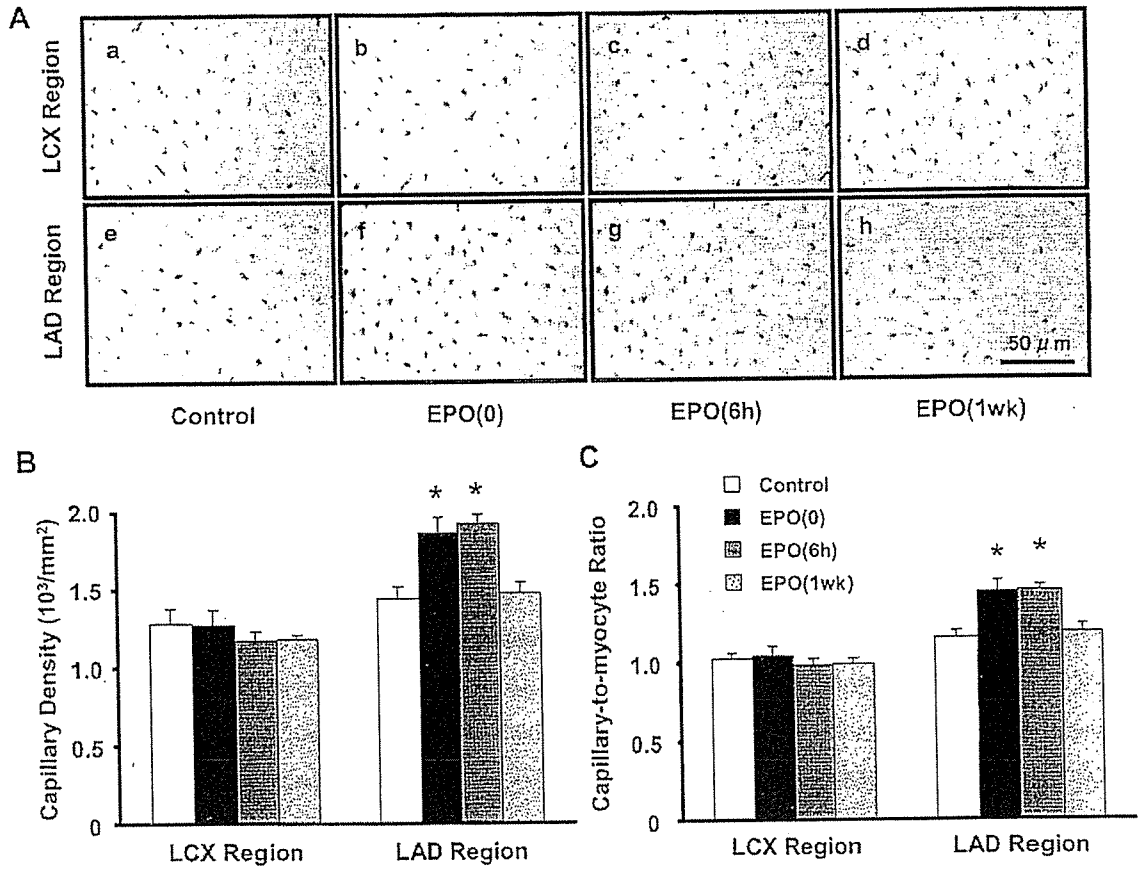

Figure 5. (A) Representative immunohistologic staining with an antibody against von Willebrand factor in nonischemic (left circumflex coronary artery [LCX]) (a, b, c, d) and ischemic (left anterior descending coronary artery [LAD]) (e, f, g, h) regions in different experimental groups. Capillary density (B) and capillary-to-myocyte ratio (C) of nonischemic (LCX) and ischemic (LAD) regions in different experimental groups. *$p < 0.05$ versus the control group. Abbreviations as in Figure 1.

EPO(0) group than in the other groups. Four weeks after MI, LVEDP was lower in the EPO(0) and EPO(6h) groups than in either the control or the EPO(1wk) group.

Myocardial infarct size 4 weeks after MI was smaller in the EPO(0) group than in the control group, although EPO treatment, initiated 6 h and 1 week after MI, did not reduce infarct size (Fig. 7D).

DISCUSSION

The present study showed that EPO administered 6 h after LAD ligation increased circulating CD34+MNCs, capillary density, MBF in the ischemic region, and prevented the worsening of cardiac function without reducing infarct size. The EPO enhances neovascularization, likely via EPC mobilization, and improves cardiac dysfunction in the chronic phase, although EPO has time-window limitations.

We showed that the EPO treatment immediately after the LAD ligation reduced infarct size, which is consistent with observations of previous reports (5–8). Because the infarct size-limiting effects of EPO appear rapidly, the nonerythroid effects of EPO, such as antiapoptosis and radical scavenging (4–8), may contribute to the reduction of infarct size.

Recent reports have shown that circulating CD34+MNC count correlated with EPC number in MNCs culture assay, and both increased at 1 to 2 weeks after EPO administration in animals and humans (9–11). In the culture assay, the number of Dil-ac-LDL/UEA-I double-positive cells obtained from blood at baseline did not differ between the two groups. The number of double-positive cells obtained from blood at 1 week after MI significantly increased compared with that at baseline in the control and EPO(0) groups. Further, the double-positive cell number obtained from blood in the EPO(0) group was higher than in the control group. These findings suggest that EPO augments increases in the number of MNCs that can differentiate into Dil-ac-LDL/UEA-I double-positive cells, an indicator of endothelial cells. Increases in the number of both CD34-positive cells and Dil-ac-LDL/UEA-I double-positive cells strongly suggest that EPO promotes EPC mobilization. The number of CD34+MNCs increased 1 week after MI in the canine model, which is consistent with observations from studies of patients with acute MI (21,22). Furthermore, the number of CD34+MNCs was higher in the EPO(0) and EPO(6h) groups than in the control group. This finding suggests that a single dose of EPO was effective in increasing the number of circulating EPCs after MI. Interestingly,

JACC Vol. 48, No. 1, 2006
July 4, 2006:176–84

EPO administered 1 week after MI failed to produce the identical effect, suggesting that EPO has a time window for promotion of EPC mobilization. We found that plasma VEGF levels were elevated, peaking at 6 h after MI and returned to the baseline 1 week after MI. The EPO did not affect plasma VEGF levels. Because both VEGF and EPO are known to promote EPC mobilization in experimental conditions and are independent predictors for the number of circulating EPCs in patients with coronary heart disease (9–11,23), they may additionally or synergistically contribute to EPC mobilization. Thus, it is likely that EPO alone, at least at the dose used in the present study, might not be enough to promote CD34+MNC mobilization 1 week after MI when VEGF returns to the baseline. Although we only investigated the low dose of EPO to consider the clinical implication, it is possible that high doses of EPO would show the different results. Further investigations are needed to clarify the mechanism of EPO-stimulated EPC mobilization.

The present study also showed that EPO increased capillary-to-myocyte ratio corrected for LV hypertrophy as well as capillary density in the EPO(0) and EPO(6h) groups, suggesting that EPO promotes the neovascularization in the ischemic region. Investigators have also reported that EPO enhances neovascularization in the ischemic region in the hind-limb occlusion model (9). As suggested in the present study, EPO may enhance neovascularization via EPC mobilization. Indeed, bone marrow-derived EPCs incorporate into foci of neovascularization at the border zone of MI (12,13), and administration of ex vivo-expanded EPCs resulted in increased myocardial neovascularization (24,25). In a rat stroke model, Wang et al. (26) showed that EPO treatment, initiated 24 h after MI, enhances angiogenesis. In addition, van der Meer et al. (27) showed that capillary density was increased in the rat post-MI model even

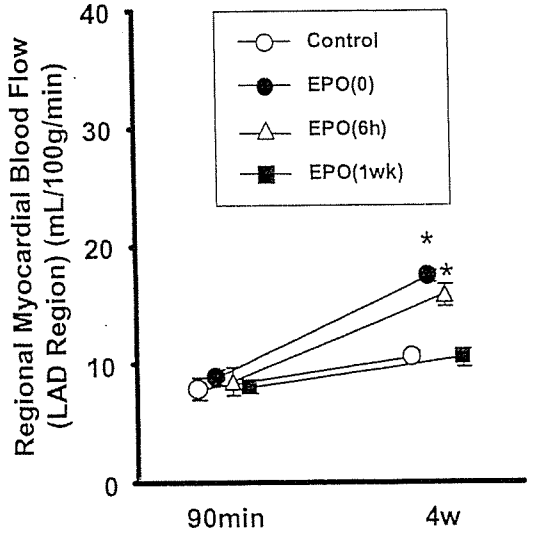

Figure 6. Regional myocardial blood flow in the ischemic (left anterior descending coronary artery [LAD]) region 90 min and 4 weeks after myocardial infarction in different experimental groups. *$p < 0.05$ versus the control group. EPO = erythropoietin.

Table 3. Time Course of Changes in Hemodynamic Parameters

Parameters	Baseline	90 Min	4 Weeks
ABP (mm Hg)			
Control	99 ± 3	101 ± 3	103 ± 2
EPO(0)	102 ± 3	99 ± 3	102 ± 2
EPO(6h)	101 ± 1	98 ± 2	101 ± 1
EPO(1wk)	102 ± 2	102 ± 3	103 ± 2
HR (per min)			
Control	131 ± 6	135 ± 6	129 ± 6
EPO(0)	128 ± 6	131 ± 3	131 ± 5
EPO(6h)	130 ± 7	135 ± 7	126 ± 6
EPO(1wk)	128 ± 6	128 ± 3	126 ± 6

Data are presented as mean ± SEM (n = 7 to 8).
ABP = arterial mean blood pressure; EPO = erythropoietin; HR = heart rate.

when EPO was administered 3 weeks after MI. In contrast, we showed that EPO administered 1 week after MI failed to increase capillary density. The possible explanation for this discrepancy is attributable to the different doses of EPO used. In the studies by Wang et al. (26) (5,000 IU/kg for 7 days) and van der Meer et al. (27) (8,000 IU/kg every 3 weeks), relatively high doses of EPO were administered. In contrast, in the present study, a relatively low dose (1,000 IU/kg) of EPO was administered with a single injection, and the reason for this dose in the present study is for the possible translation of our results to clinical settings more easily (6), because 8,000 or 5,000 IU/kg EPO may cause side effects. On the other hand, we noticed that a higher dose of EPO would increase capillary density and improve the cardiac function even by the late administration of EPO for clinical use.

In the present study, MBF in the ischemic region was increased in both the EPO(0) and the EPO(6h) groups. Because neovascularization was also enhanced in these groups, increased MBF may occur secondary to the enhanced neovascularization.

The present study also showed that an administration of EPO immediately after the LAD ligation improved cardiac function at 90 min after MI, likely because of infarct size reduction, and subsequently prevented the development of cardiac dysfunction in the chronic phase. Because the previous reports showed that myocardial necrosis progresses within 6 h after the onset of MI (28,29), EPO was administered at time points of 6 h and later after LAD ligation to determine whether its activity is directed toward the acute phase of MI or the chronic phase of cardiac dysfunction. One week after MI, LVEF, LVEDD, or LVEDP was similar among the EPO(6h), EPO(1wk), and control groups. However, EPO administered 6 h, but not 1 week, after the LAD ligation improved cardiac dysfunction 4 weeks after MI when compared with the control group. Because we did not find any difference in infarct size at 4 weeks after MI between the EPO(6h) and the EPO(1wk) groups, the improvement of cardiac function in the EPO(6h) group was not attributable to the reduction of infarct size, but to the increased blood flow to the ischemic regions.

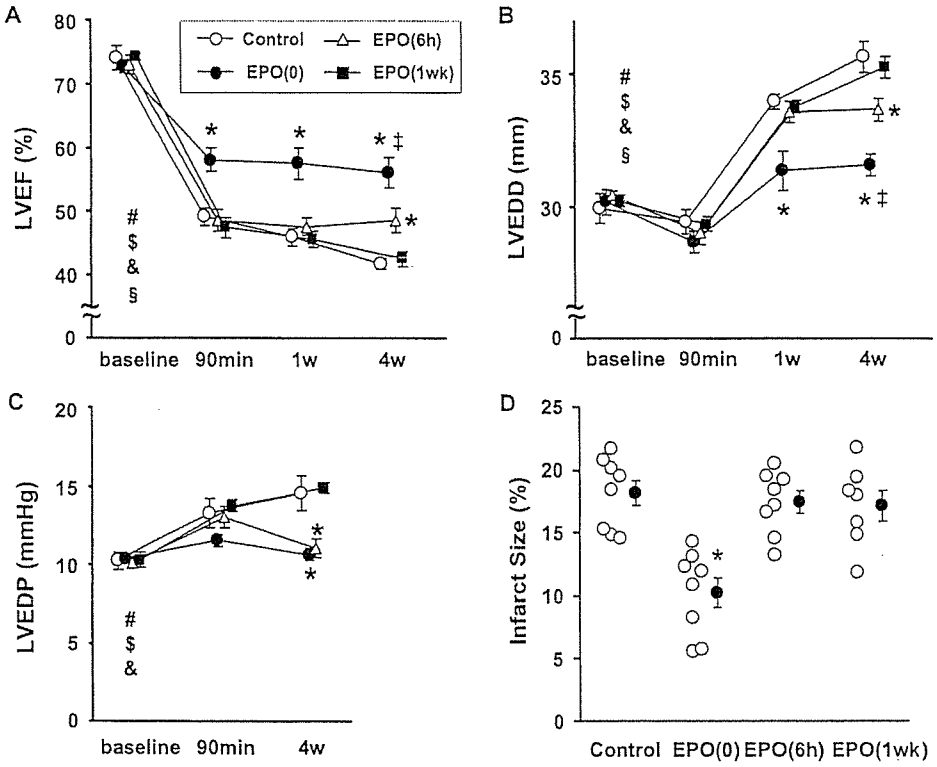

Figure 7. The time course of changes in left ventricular ejection fraction (LVEF) (A), left ventricular end-diastolic dimension (LVEDD) (B), and left ventricular end-diastolic pressure (LVEDP) (C) in different experimental groups. Statistically significant ($p < 0.05$) group-by-time interactions (analysis of variance for repeated measurements) are indicated by the following: # = all groups; $ = control × EPO(0) group; & = control × EPO(6h) group; § = EPO(0) × EPO(6h) group. (D) Infarct size at 4 weeks after myocardial infarction in different experimental groups. Open circles = infarct size in each animal. *$p < 0.05$ versus the control group. EPO = erythropoietin.

In conclusion, in addition to its acute effect on infarct size reduction, EPO may exert chronic cardioprotective effects through neovascularization and may be a useful adjunct for the treatment of patients with myocardial infarction.

Acknowledgments

The authors thank Hiroko Okuda, Akiko Ogai, Yoko Nagamachi, and Nobuko Kawasaki for their technical assistance.

Reprint requests and correspondence: Dr. Tetsuo Minamino, Department of Cardiovascular Medicine, Osaka University Graduate School of Medicine, 2-2 Yamadaoka, Suita, Osaka 565-0871, Japan. E-mail: minamino@medone.med.osaka-u.ac.jp.

REFERENCES

1. Krantz SB. Erythropoietin. Blood 1991;77:419–34.
2. Cotter DJ, Thamer M, Kimmel PL, Sadler JH. Secular trends in recombinant erythropoietin therapy among the U.S. hemodialysis population: 1990–1996. Kidney Int 1998;54:2129–39.
3. Sakanaka M, Wen TC, Matsuda S, et al. In vivo evidence that erythropoietin protects neurons from ischemic damage. Proc Natl Acad Sci U S A 1998;95:4635–40.
4. Chattopadhyay A, Choudhury TD, Bandyopadhyay D, Datta AG. Protective effect of erythropoietin on the oxidative damage of erythrocyte membrane by hydroxyl radical. Biochem Pharmacol 2000;59:419–25.
5. Moon C, Krawczyk M, Ahn D, et al. Erythropoietin reduces myocardial infarction and left ventricular functional decline after coronary artery ligation in rats. Proc Natl Acad Sci U S A 2003;100:11612–7.
6. Hirata A, Minamino T, Asanuma H, et al. Erythropoietin just before reperfusion reduces both lethal arrhythmias and infarct size via the phosphatidylinositol-3 kinase-dependent pathway in canine hearts. Cardiovasc Drugs Ther 2005;19:33–40.
7. Parsa CJ, Matsumoto A, Kim J, et al. A novel protective effect of erythropoietin in the infarcted heart. J Clin Invest 2003;112:999–1007.
8. Lipsic E, van der Meer P, Henning RH, et al. Timing of erythropoietin treatment for cardioprotection in ischemia/reperfusion. J Cardiovasc Pharmacol 2004;44:473–9.
9. Heeschen C, Aicher A, Lehmann R, et al. Erythropoietin is a potent physiologic stimulus for endothelial progenitor cell mobilization. Blood 2003;102:1340–6.
10. Bahlmann FH, DeGroot K, Duckert T, et al. Endothelial progenitor cell proliferation and differentiation is regulated by erythropoietin. Kidney Int 2003;64:1648–52.
11. Bahlmann FH, De Groot K, Spandau JM, et al. Erythropoietin regulates endothelial progenitor cells. Blood 2004;103:921–6.
12. Asahara T, Masuda H, Takahashi T, et al. Bone marrow origin of endothelial progenitor cells responsible for postnatal vasculogenesis in physiological and pathological neovascularization. Circ Res 1999;85:221–8.
13. Asahara T, Murohara T, Sullivan A, et al. Isolation of putative progenitor endothelial cells for angiogenesis. Science 1997;275:964–7.
14. Kitakaze M, Hori M, Morioka T, et al. Alpha 1-adrenoceptor activation mediates the infarct size-limiting effect of ischemic preconditioning through augmentation of 5'-nucleotidase activity. J Clin Invest 1994;93:2197–205.
15. Koumegawa J, Kawahara J, Kubo K, et al. Recombinant human erythropoietin corrects anemia of blood loss: a study in the dog. Int J Cell Cloning 1990;8:97–106.
16. Clifford CA, Hughes D, Beal MW, et al. Plasma vascular endothelial growth factor concentrations in healthy dogs and dogs with hemangiosarcoma. J Vet Intern Med 2001;15:131–5.
17. Horrigan MC, MacIsaac AI, Nicolini FA, et al. Reduction in myocardial infarct size by basic fibroblast growth factor after

temporary coronary occlusion in a canine model. Circulation 1996;94:1927–33.
18. Pu Q, Larouche I, Schiffrin EL. Effect of dual angiotensin converting enzyme/neutral endopeptidase inhibition, angiotensin converting enzyme inhibition, or AT1 antagonism on coronary microvasculature in spontaneously hypertensive rats. Am J Hypertens 2003;16:931–7.
19. Mori H, Haruyama S, Shinozaki Y, et al. New nonradioactive microspheres and more sensitive x-ray fluorescence to measure regional blood flow. Am J Physiol 1992;263:H1946–57.
20. Holm S. A simple sequentially rejective multiple test procedure. Scand J Stat 1979;6:65–70.
21. Shintani S, Murohara T, Ikeda H, et al. Mobilization of endothelial progenitor cells in patients with acute myocardial infarction. Circulation 2001;103:2776–9.
22. Massa M, Rosti V, Ferrario M, et al. Increased circulating hematopoietic and endothelial progenitor cells in the early phase of acute myocardial infarction. Blood 2005;105:199–206.
23. Asahara T, Takahashi T, Masuda H, et al. VEGF contributes to postnatal neovascularization by mobilizing bone marrow-derived endothelial progenitor cells. Embo J 1999;18:3964–72.
24. Kocher AA, Schuster MD, Szabolcs MJ, et al. Neovascularization of ischemic myocardium by human bone-marrow-derived angioblasts prevents cardiomyocyte apoptosis, reduces remodeling and improves cardiac function. Nat Med 2001;7:430–6.
25. Kawamoto A, Gwon HC, Iwaguro H, et al. Therapeutic potential of ex vivo expanded endothelial progenitor cells for myocardial ischemia. Circulation 2001;103:634–7.
26. Wang L, Zhang Z, Wang Y, Zhang R, Chopp M. Treatment of stroke with erythropoietin enhances neurogenesis and angiogenesis and improves neurological function in rats. Stroke 2004;35:1732–7.
27. van der Meer P, Lipsic E, Henning RH, et al. Erythropoietin induces neovascularization and improves cardiac function in rats with heart failure after myocardial infarction. J Am Coll Cardiol 2005;46:125–33.
28. Reimer KA, Lowe JE, Rasmussen MM, Jennings RB. The wavefront phenomenon of ischemic cell death. 1. Myocardial infarct size vs duration of coronary occlusion in dogs. Circulation 1977;56:786–94.
29. Hirayama A, Adachi T, Asada S, et al. Late reperfusion for acute myocardial infarction limits the dilatation of left ventricle without the reduction of infarct size. Circulation 1993;88:2565–74.

Available online at www.sciencedirect.com

SCIENCE DIRECT

Life Sciences 78 (2006) 882 – 887

Life Sciences

www.elsevier.com/locate/lifescie

Vagal stimulation suppresses ischemia-induced myocardial interstitial norepinephrine release

Toru Kawada [a,*], Toji Yamazaki [b], Tsuyoshi Akiyama [b], Meihua Li [a], Hideto Ariumi [a], Hidezo Mori [b], Kenji Sunagawa [c], Masaru Sugimachi [a]

[a] *Department of Cardiovascular Dynamics, Advanced Medical Engineering Center, National Cardiovascular Center Research Institute, 5-7-1 Fujishirodai, Suita, Osaka 565-8565, Japan*

[b] *Department of Cardiac Physiology, National Cardiovascular Center Research Institute, Osaka 565-8565, Japan*

[c] *Department of Cardiovascular Medicine, Graduate School of Medical Sciences, Kyushu University, Fukuoka 812-8582, Japan*

Received 30 November 2004; accepted 31 May 2005

Abstract

Although electrical vagal stimulation exerts beneficial effects on the ischemic heart such as an antiarrhythmic effect, whether it modulates norepinephrine (NE) and acetylcholine (ACh) releases in the ischemic myocardium remains unknown. To clarify the neural modulation in the ischemic region during vagal stimulation, we examined ischemia-induced NE and ACh releases in anesthetized and vagotomized cats. In a control group (VX, $n=8$), occlusion of the left anterior descending coronary artery increased myocardial interstitial NE level from 0.46±0.09 to 83.2±17.6 nM at 30–45 min of ischemia (mean±SE). Vagal stimulation at 5 Hz (VS, $n=8$) decreased heart rate by approximately 80 beats/min during the ischemic period and suppressed the NE release to 24.4±10.6 nM ($P<0.05$ from the VX group). Fixed-rate ventricular pacing (VSP, $n=8$) abolished this vagally mediated suppression of ischemia-induced NE release. The vagal stimulation augmented ischemia-induced ACh release at 0–15 min of ischemia (VX: 11.1±2.1 vs. VS: 20.7±3.9 nM, $P<0.05$). In the VSP group, the ACh release was not augmented. In conclusion, vagal stimulation suppressed the ischemia-induced NE release and augmented the initial increase in the ACh level. These modulations of NE and ACh levels in the ischemic myocardium may contribute to the beneficial effects of vagal stimulation on the heart during acute myocardial ischemia.

Keywords: Acetylcholine; Coronary occlusion; Ventricular pacing

Introduction

Acute myocardial ischemia disrupts normal neural regulation of the heart (Armour, 1999). During prolonged ischemia, myocardial interstitial norepinephrine (NE) and acetylcholine (ACh) levels are increased in the ischemic region via local releasing mechanisms independent of efferent autonomic activities (Schömig et al., 1987; Lameris et al., 2000; Kawada et al., 2000, 2001). The excess NE release is thought to aggravate ischemic injury to the myocardium (Schömig et al., 1987). On the other hand, vagal stimulation exerts antiarrhythmic effects in the early phase of acute myocardial ischemia (Rosenshtraukh et al., 1994; Vanoli et al., 1991). A recent study from our laboratory demonstrated that vagal stimulation improved the survival rate of chronic heart failure after myocardial infarction in rats (Li et al., 2004), suggesting a long-term ameliorative effect of direct neural interventions against certain heart diseases.

With respect to electrical stimulation of the vagus, whether it alters myocardial interstitial NE and ACh levels in the ischemic region during acute myocardial ischemia remains unknown. To test the hypothesis that vagal stimulation increases the ACh level and suppresses the NE level in the ischemic region, we measured myocardial interstitial NE and ACh levels during acute myocardial ischemia in anesthetized cats using a cardiac microdialysis technique (Akiyama et al., 1991, 1994; Yamazaki et al., 1997). Effects of vagal stimulation were examined with or without fixed-rate ventricular pacing.

* Corresponding author. Tel.: +81 6 6833 5012x2427; fax: +81 6 6835 5403.
E-mail address: torukawa@res.ncvc.go.jp (T. Kawada).

0024-3205/$ - see front matter © 2005 Elsevier Inc. All rights reserved.
doi:10.1016/j.lfs.2005.05.087

Materials and methods

This investigation conforms with the *Guide for the Care and Use of Laboratory Animals* published by the US National Institutes of Health (NIH Publication No. 85-23, revised 1996).

Surgical preparation

Twenty-four adult cats weighing from 2.2 to 3.8 kg were anesthetized by an intraperitoneal injection of pentobarbital sodium (30–35 mg/kg) and ventilated mechanically with room air mixed with oxygen. The depth of anesthesia was maintained with a continuous intravenous infusion of pentobarbital sodium (1–2 mg kg^{-1} h^{-1}) through a catheter inserted from the right femoral vein to the inferior vena cava. Systemic arterial pressure (AP) was monitored from a catheter inserted from the right femoral artery into the abdominal aorta. Heart rate (HR) was determined from an electrocardiogram using a cardiotachometer. Esophageal temperature of the animal was measured using a thermometer (CTM-303, TERUMO, Japan) and was maintained at around 37 °C using a heated pad and a lamp.

Bilateral vagal nerves were sectioned through a midline cervical incision. With the animal in the lateral position, the left fifth and sixth ribs were resected to expose the heart. A dialysis probe was implanted, using a fine guiding needle, into the anterolateral free wall of the left ventricle perfused by the left anterior descending coronary artery (LAD). A 3-0 silk suture was passed around the LAD just distal to the first diagonal branch for later coronary occlusion. When an experimental protocol required electrical stimulation of the vagal efferent nerves, bipolar platinum electrodes were attached to the cardiac end of sectioned vagal nerves bilaterally. The nerves and electrodes were covered with warmed mineral oil for insulation. When an experimental protocol required cardiac pacing, bipolar stainless-steel wire electrodes were sutured at the left ventricular apex away from the implanted dialysis probe. Heparin sodium (100 U/kg) was administered intravenously to prevent blood coagulation.

In additional four anesthetized cats, the left ventricle was implanted with a dialysis probe and a pair of pacing electrodes to examine the effects of left ventricular pacing alone on the myocardial interstitial NE levels. The dialysis probe and pacing leads were placed in the same manner as described in the previous paragraph.

At the end of the experiment, the experimental animals were killed with an overdose of pentobarbital sodium. Postmortem examination confirmed that the dialysis probe had been implanted within the left ventricular myocardium.

Dialysis technique

The materials and properties of the dialysis probe have been previously described (Akiyama et al., 1991, 1994). Briefly, we designed a transverse dialysis probe. A dialysis fiber (13 mm length, 310 μm O.D., 200 μm I.D.; PAN-1200, 50,000 molecular weight cutoff, Asahi Chemical, Japan) was glued at both ends to polyethylene tubes (25 cm length, 500 μm O.D., 200 μm I.D.). The dialysis probe was perfused at a rate of 2 μl/min with Ringer solution containing the cholinesterase inhibitor eserine (100 μM). Dialysate sampling was initiated 2 h after implanting the dialysis probe, when the dialysate concentrations of NE and ACh had reached steady states (Akiyama et al., 1991, 1994). The actual dialysate sampling lagged behind a given collection period by 5 min taking into account the dead space volume between the dialysis membrane and the sample tube. Dialysate concentrations of NE and ACh were measured separately by high performance liquid chromatography with electrochemical detection (DTA-300, Eicom, Japan). Details of the NE and ACh measurements have been previously described (Akiyama et al., 1991, 1994).

Protocols

Protocol 1 (VX, n = 8)

As a control experiment, we measured ischemia-induced NE and ACh releases during 60-min LAD occlusion in vagotomized animals. After collecting a 15-min baseline dialysate sample, we occluded the LAD for 60 min and collected four consecutive 15-min dialysate samples during acute myocardial ischemia. We then loosened the LAD snare and collected a 15-min dialysate sample during reperfusion.

Protocol 2 (VS, n = 8)

We examined the effects of vagal stimulation on ischemia-induced NE and ACh releases. To avoid possible preconditioning mimetic effects of ACh released by vagal stimulation (Przyklenk and Kloner, 1995; Kawada et al., 2002a), we initiated the bilateral vagal stimulation (5 Hz, 1 ms in pulse duration and 10 V in pulse amplitude) at the onset of LAD occlusion. The vagal stimulation continued for the 60-min ischemic period and the 15-min reperfusion period.

Protocol 3 (VSP, n = 8)

To eliminate the effects of bradycardia associated with vagal stimulation, we performed vagal stimulation under fixed-rate pacing conditions. We initiated the bilateral vagal stimulation (5 Hz, 1 ms in pulse duration and 10 V in pulse amplitude) and paced the heart from the onset of LAD occlusion to the conclusion of the experimental period. The ventricular pacing rate was set close to the HR recorded immediately before the LAD occlusion.

Supplemental protocol (n = 4)

To examine the effects of left ventricular pacing on the myocardial interstitial NE levels, we collected 15-min dialysate samples under control conditions as well as under left ventricular pacing at 170 beats/min.

Statistical analysis

All data are presented as means ± SE values. In each group, the effects of LAD occlusion on dialysate concentrations of NE and ACh were examined using a repeated-measures analysis of

variance followed by a Dunnett test against respective baseline concentrations. Because the variance of NE data was very large and increased with mean, the NE data were compared after the logarithmic transform (Snedecor and Cochran, 1989). Differences were considered significant at $P<0.05$. To examine the effects of vagal stimulation with or without the ventricular pacing, dialysate concentrations of NE and ACh were compared among the three groups at each corresponding time period using one-way analysis of variance followed by a Student–Newman–Keuls test for all pairwise comparisons (Glantz, 2002). The NE data were compared after the logarithmic transform. Differences were considered significant at $P<0.05$. Heart rate and mean AP were determined immediately before the coronary occlusion (designated as time 0), after 5, 10, 15, 30, 45, and 60 min of the occlusion, and after 15 min of reperfusion. One-way analysis of variance followed by a Student–Newman–Keuls test was also applied to compare HR and mean AP among the three groups at each time point.

Results

Fig. 1 depicts LAD occlusion-induced myocardial interstitial NE accumulation within the ischemic zone. The inset shows the NE levels during baseline conditions in a magnified ordinate. In the VX group, LAD occlusion increased the NE level approximately 200 fold compared to the baseline level at 45–60 min. This occlusion-induced NE accumulation was significantly suppressed in the VS group compared with the VX group in 15–30, 30–45, and 45–60 min time periods. The difference between the VS and VX groups did not reach statistical significance at the reperfusion period. In the VSP group, in which HR was kept constant, vagal stimulation did not attenuate the occlusion-induced NE accumulation. In the supplemental protocol, the baseline myocardial interstitial NE level was 0.17±0.01 nM. The NE level during ventricular pacing at 170 beats/min was 0.21±0.09 nM.

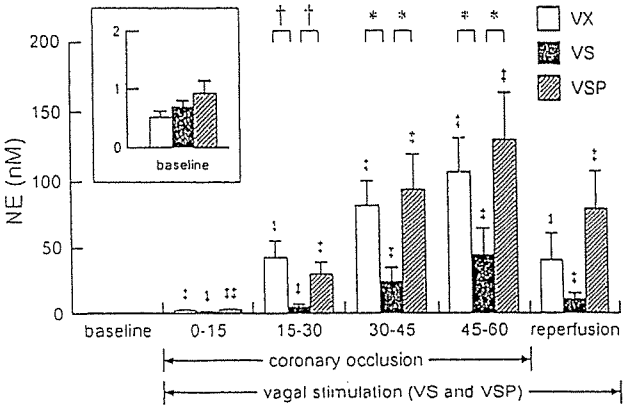

Fig. 1. Coronary occlusion-induced norepinephrine (NE) accumulation in the ischemic myocardium. VX: vagotomy, VS: vagal stimulation, VSP: vagal stimulation with ventricular pacing. The inset shows the baseline conditions with a magnified ordinate. Data are means±SE. ‡$P<0.01$ and ‡‡$P<0.05$ from the corresponding baseline value in each group. †$P<0.01$ and *$P<0.05$ by all pairwise comparisons among the three groups.

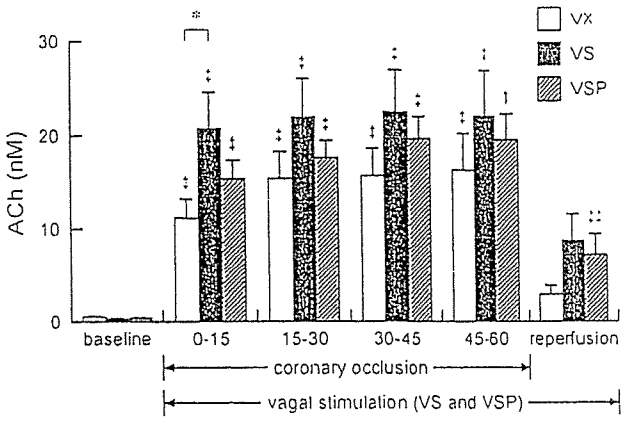

Fig. 2. Coronary occlusion-induced acetylcholine (ACh) accumulation in the ischemic myocardium. Data are means±SE. ‡$P<0.01$ and ‡‡$P<0.05$ from the corresponding baseline value in each group. *$P<0.05$ by all pairwise comparisons among the three groups.

Fig. 2 shows LAD occlusion-induced myocardial interstitial ACh accumulation within the ischemic zone. In the VX group, LAD occlusion increased the ACh level approximately 20 times higher than the baseline level at 45–60 min. The ACh level at 0–15 min was significantly higher in the VS than the VX group. For the rest of the ischemic period and reperfusion period, the differences between the VS and VX groups were not significant. The ACh levels in the VSP group did not differ from the VX group for any of the sampling periods.

Fig. 3 summarizes changes in HR and mean AP. In the VS group, HR was decreased by approximately 80 beats/min compared with the VX group at 5 min of coronary occlusion. The HR decrease continued for the rest of the ischemic period and reperfusion period. In the VSP group, HR was kept close to the preocclusion level, and it did not differ from the VX group

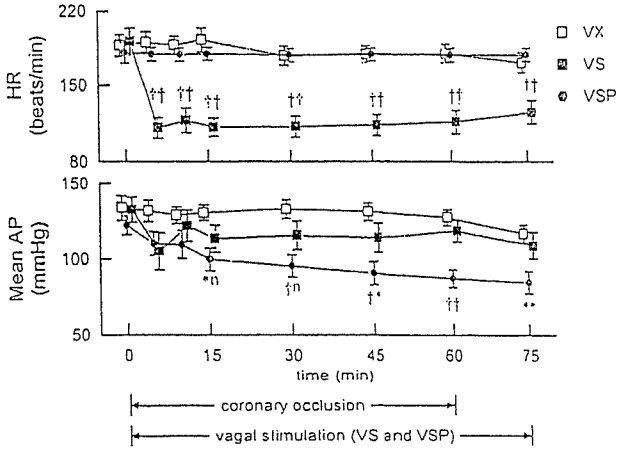

Fig. 3. Time courses of heart rate (HR) and mean arterial pressure (AP) during 60-min ischemia and 15-min reperfusion. The baseline values obtained just before coronary occlusion are plotted at time 0. Data points for VX and VSP groups are slightly displaced along the time axis for better view of overlapping points. Data are means±SE. In the HR data, †† represents statistical significance of $P<0.01$ from both the VX and VSP groups by all pairwise comparisons. In the AP data, when two characters are added to the VSP data point, the first and second characters represent the statistical significance from VX and VS groups, respectively. *, †, and n designate $P<0.05$, $P<0.01$, and "not significant", respectively.

for all the time points. Mean AP did not differ statistically between VX and VS groups. Mean AP in the VSP group progressively decreased and became significantly lower than the VX group after 15 min of the ischemic period. Mean AP in the VSP group was also significantly lower than the VS group after 45 min of the ischemic period.

Discussion

We have shown that electrical vagal stimulation suppressed ischemia-induced NE release and enhanced an initial increase in the ACh levels in the ischemic myocardium. Fixed-rate pacing abolished the suppression of ischemia-induced NE release by vagal stimulation in the present experimental settings.

Effects of vagal stimulation on ischemia-induced NE release

Several mechanisms can be put forward to explain the suppression of ischemia-induced myocardial interstitial NE release by vagal stimulation. First, activation of presynaptic muscarinic receptors on the sympathetic nerve endings inhibits the exocytotic NE release under normal physiological conditions (Levy and Blattberg, 1976). However, the presynaptic inhibition is unlikely the mechanism underlying the vagally mediated suppression of the ischemia-induced NE release because of the following reasons. Although the exocytotic release mechanism participates in the ischemia-induced NE release within the first 20 min of ischemia, the non-exocytotic release mechanism becomes predominant as the ischemic period is prolonged (Akiyama and Yamazaki, 1999). Myocardial ischemia gradually depletes ATP in the ischemic region including sympathetic nerve terminals, which leads to accumulation of axoplasmic NE and reduction of normal Na^+gradient across the plasma membrane in the sympathetic nerve terminals. The NE uptake transporter on the sympathetic nerve terminals, driven by the Na^+gradient, is then reversed, evoking non-exocytotic NE release (Schwartz, 2000). Therefore, the presynaptic inhibition of exocytotic NE release might contribute little to the suppression of ischemia-induced NE release during prolonged ischemia. Furthermore, the presynaptic inhibition of exocytotic NE release becomes less effective during the ischemic insult (Du et al., 1990; Haunstetter et al., 1994). The fact that the ischemia-induced NE release did not differ between the VSP and VX groups is also in opposition to the presynaptic inhibition as a chief mechanism underlying the vagally mediated suppression of ischemia-induced NE release (Fig. 1). Although left ventricular pacing could have affected myocardial interstitial NE levels, the results of the supplemental protocol indicates that changes in the NE levels by ventricular pacing might be negligibly small compared to the ischemia-induced NE release.

Second, the suppression of ischemia-induced NE release by vagal stimulation may be related to myocardial protection via direct vasodiation of the coronary artery. The coronary dilation may enhance collateral flow in the ischemic region and protect against myocardial deterioration evoked by ischemia. Both ACh and vasoactive intestinal polypeptide (VIP) are known to exert direct coronary dilation (Feliciano and Henning, 1998; Gross et al., 1981; Henning and Sawmiller, 2001). VIP is colocalized with ACh in the postganglionic vagal fibers and is released by high-frequency (20 Hz) vagal stimulation. VIP may interact with NE transport or exocytosis like nociceptin (Yamazaki et al., 2001). However, fixed-rate pacing abolished the ability of vagal stimulation to suppress the ischemia-induced NE release. Hence the direct coronary vasodilation and/or interaction with the sympathetic system via VIP might have played little role in suppressing ischemia-induced NE release in the present experimental settings. Another factor that should be taken into account is that the relatively low-frequency (5 Hz) stimulation might have limited the amount of VIP release from the vagal nerve endings.

Third, HR is one of the most important determinants of myocardial oxygen consumption (Mohrman and Heller, 1997). In the present study, HR in the VS group decreased to approximately 60% that of the VX group during the ischemic period (Fig. 3), which slowed the energy consumption of the myocardium. Bradycardia might also decrease ventricular contractility via a force-frequency mechanism (Maughan et al., 1985). In addition, bradycardia may increase coronary perfusion via prolongation of diastolic interval (Buck et al., 1981). These factors slowed energy consumption in the ischemic region including sympathetic nerve terminals, delaying the time course for non-exocytotic NE release. The prevention of excess NE would further reduce myocardial oxygen consumption and decelerate the progression of ischemic injury (Suga et al., 1983). The ischemia-induced NE release did not differ between the VSP and VX groups despite the lower mean AP in the VSP compared with the VX group. Although lowering AP might decrease afterload of the ventricle and reduce energy consumption, the beneficial effect of afterload reduction might have been masked in the VSP group due to inefficient cardiac pumping function associated with asynchrony between sinus rate and ventricular rate. Proper atrioventricular conduction time contributes to the ventricular filling (Meisner et al., 1985). In the VSP group, the sinus rate was reduced by vagal stimulation whereas the ventricular rate was maintained by fixed-rate pacing. Dissociation of the sinus rate and ventricular rate might have impaired the ventricular filling to a variable extent, resulting in a progressive reduction in AP.

Finally, the vagal stimulation decreases ventricular contractile force against sympathetic activation via the direct projections to the ventricle (Nakayama et al., 2001). This mechanism might have also contributed to the reduction of the myocardial oxygen consumption and slowed the progression of ischemic injury in the VS group. However, the ventricular pacing canceled the protective effects in the VSP group, possibly by the adverse influences discussed in the previous paragraph. Further studies are required to isolate the factor(s) most important for the suppression of ischemia-induced NE release by the vagal stimulation.

Effects of vagal stimulation on ischemia-induced ACh release

In contrast to the suppressive effect of NE release, vagal nerve stimulation can exert two opposing influences on ACh release in the ischemic myocardium. The nerve stimulation itself induces exocytotic ACh release from nerve endings. Acute myocardial ischemia impairs conduction of the nerves traversing in the ischemic region (Barber et al., 1983; Inoue and Zipes, 1988; Martins et al., 1989). Acute myocardial ischemia also impairs the exocytotic ACh release in the postischemic myocardium (Kawada et al., 2002b). On the other hand, acute myocardial ischemia causes myocardial ACh release in the ischemic region via a local release mechanism independent of efferent nerve activity (Kawada et al., 2000). Hence, the amount of ACh release was net effects of ACh release evoked by nerve stimulation and ischemia; vagally mediated protection against ischemic injury should augment the former and attenuate the latter.

Although vagal stimulation augmented myocardial interstitial ACh release during the 0–15 min period of coronary occlusion in the VS group than in the VX group, the initial enhancement was not observed in the VSP group. One possible mechanism for the difference in the initial ACh release between the VS and VSP groups is that the progression of ischemia in the VSP group relative to the VS group impaired the vagal nerve conduction in the ischemic region, reducing the exocytotic ACh release. The other possible mechanism is that the high levels of NE might have attenuated the stimulation-induced ACh release from the vagal nerve endings via α-adrenergic mechanisms (Akiyama and Yamazaki, 2000).

There are several limitations to the present study. First, we avoided large myocardial ischemia by occluding LAD just distal to the first diagonal branch. Accordingly, the incidence of lethal ventricular arrhythmia was too low to draw any conclusion as to the effects of vagal stimulation on the arrhythmogenesis. Further studies with larger myocardial ischemia are clearly required to examine the effects of vagal stimulation on the incidence of lethal ventricular arrhythmia in relation to the observed NE and/or ACh levels in the ischemic myocardium. Second, plasma catecolamine levels might have been increased during the LAD occlusion, which might affect HR and cardiac function in the non-ischemic region. Although changes in plasma catecholamine levels may play significant roles in determining systemic hemodynamics, the ischemic region was only poorly perfused. Accordingly, direct effects of plasma catecholamines on the myocardial interstitial NE and ACh levels in the ischemic region might have been limited in the present study.

Conclusion

Electrical vagal stimulation suppressed ischemia-induced NE release in the ischemic myocardium in anesthetized cats. The vagal stimulation augmented ischemia-induced ACh release at the 0–15 min period of ischemia. Although acute myocardial ischemia causes myocardial NE and ACh releases independent of efferent nerve activity, the vagal stimulation was able to modulate both NE and ACh levels in the ischemic region. The suppression of NE release and augmentation of initial ACh release in the ischemic myocardium by vagal stimulation may reduce the ischemic injury to the heart. The direct neural intervention could be a new modality of medical engineering to cope with ischemic heart diseases.

Acknowledgments

This study was supported by Health and Labour Sciences Research Grant for Research on Advanced Medical Technology (H14-Nano-002) from the Ministry of Health Labour and Welfare of Japan, by Grant-in-Aid for Scientific Research (C-15590786) from the Ministry of Education, Science, Sports and Culture of Japan, and by the Program for Promotion of Fundamental Studies in Health Science from the Organization for Pharmaceutical Safety and Research.

References

Akiyama, T., Yamazaki, T., 1999. Norepinephrine release from cardiac sympathetic nerve endings in the in vivo ischemic region. Journal of Cardiovascular Pharmacology 34, S11–S14.

Akiyama, T., Yamazaki, T., 2000. Adrenergic inhibition of endogenous acetylcholine release on postganglionic cardiac vagal nerve terminals. Cardiovascular Research 46, 531–538.

Akiyama, T., Yamazaki, T., Ninomiya, I., 1991. In vivo monitoring of myocardial interstitial norepinephrine by dialysis technique. American Journal of Physiology. Heart and Circulatory Physiology 261, H1643–H1647.

Akiyama, T., Yamazaki, T., Ninomiya, I., 1994. In vivo detection of endogenous acetylcholine release in cat ventricles. American Journal of Physiology. Heart and Circulatory Physiology 266, H854–H860.

Armour, J.A., 1999. Myocardial ischaemia and the cardiac nervous system. Cardiovascular Research 41, 41–54.

Barber, M.J., Mueller, T.M., Henry, D.P., Felten, S.Y., Zipes, D.P., 1983. Transmural myocardial infarction in the dog produces sympathectomy in noninfarcted myocardium. Circulation 67, 787–796.

Buck, J.D., Warltier, D.C., Hardman, H.F., Gross, G.J., 1981. Effects of sotalol and vagal stimulation on ischemic myocardial blood flow distribution in the canine heart. Journal of Pharmacological and Experimental Therapeutics 216, 347–351.

Du, X.J., Dart, A.M., Riemersma, R.A., Oliver, M.F., 1990. Failure of the cholinergic modulation of norepinephrine release during acute myocardial ischemia in the rat. Circulation Research 66, 950–956.

Feliciano, L., Henning, R.J., 1998. Vagal nerve stimulation releases vasoactive intestinal peptide which significantly increases coronary artery blood flow. Cardiovascular Research 40, 45–55.

Glantz, S.A., 2002. Primer of Biostatistics, 5th ed. McGraw-Hill, New York.

Gross, G.J., Buck, J.D., Warltier, D.C., 1981. Transmural distribution of blood flow during activation of coronary muscarinic receptors. American Journal of Physiology. Heart and Circulatory Physiology 240, H941–H946.

Haunstetter, A., Haass, M., Yi, X., Krüger, C., Kübler, W., 1994. Muscarinic inhibition of cardiac norepinephrine and neuropeptide Y release during ischemia and reperfusion. American Journal of Physiology. Regulatory, Integrative and Comparative Physiology 267, R1552–R1558.

Henning, R.J., Sawmiller, D.R., 2001. Vasoactive intestinal peptide: cardiovascular effects. Cardiovascular Research 49, 27–37.

Inoue, H., Zipes, D.P., 1988. Time course of denervation of efferent sympathetic and vagal nerves after occlusion of the coronary artery in the canine heart. Circulation Research 62, 1111–1120.

Kawada, T., Yamazaki, T., Akiyama, T., Sato, T., Shishido, T., Inagaki, M., Takaki, H., Sugimachi, M., Sunagawa, K., 2000. Differential acetylcholine release mechanisms in the ischemic and non-ischemic myocardium. Journal of Molecular and Cellular Cardiology 32, 405–414.

Kawada, T., Yamazaki, T., Akiyama, T., Inagaki, M., Shishido, T., Zheng, C., Yanagiya, Y., Sugimachi, M., Sunagawa, K., 2001. Vagosympathetic interactions in ischemia-induced myocardial norepinephrine and acetylcholine release. American Journal of Physiology. Heart and Circulatory Physiology 280, H216–H221.

Kawada, T., Yamazaki, T., Akiyama, T., Mori, H., Inagaki, M., Shishido, T., Takaki, H., Sugimachi, M., Sunagawa, K., 2002. Effects of brief ischaemia on myocardial acetylcholine and noradrenaline levels in anaesthetized cats. Autonomic Neuroscience 95, 37–42.

Kawada, T., Yamazaki, T., Akiyama, T., Mori, H., Uemura, K., Miyamoto, T., Sugimachi, M., Sunagawa, K., 2002. Disruption of vagal efferent axon and nerve terminal function in the postischemic myocardium. American Journal of Physiology. Heart and Circulatory Physiology 283, H2687–H2691.

Lameris, T.W., de Zeeuw, Sandra, Alberts, G., Boomsma, F., Duncker, D.J., Verdouw, P.D., Veld, A.J., van den Meiracker, A.H., 2000. Time course and mechanism of myocardial catecholamine release during transient ischemia in vivo. Circulation 101, 2645–2650.

Levy, M.N., Blattberg, B., 1976. Effect of vagal stimulation on the overflow of norepinephrine into the coronary sinus during cardiac sympathetic nerve stimulation in the dog. Circulation Research 38, 81–84.

Li, M., Zheng, C., Sato, T., Kawada, T., Sugimachi, M., Sunagawa, K., 2004. Vagal nerve stimulation markedly improves long-term survival after chronic heart failure in rats. Circulation 109, 120–124.

Martins, J.B., Lewis, R., Wendt, D., Lund, D.D., Schmid, P.G., 1989. Subendocardial infarction produces epicardial parasympathetic denervation in canine left ventricle. American Journal of Physiology. Heart and Circulatory Physiology 256, H859–H866.

Maughan, W.L., Sunagawa, K., Burkhoff, D., Graves, W.L. Jr., Hunter, W.C., Sagawa, K., 1985. Effect of heart rate on the canine end-systolic pressure–volume relationship. Circulation 72, 654–659.

Meisner, J.S., McQueen, D.M., Ishida, Y., Vetter, H.O., Bortolotti, U., Strom, J.A., Frater, R.W.M., Peskin, C.S., Yellin, E.L., 1985. Effects of timing of atrial systole on LV filling and mitral valve closure: computer and dog studies. American Journal of Physiology. Heart and Circulatory Physiology 249, H604–H619.

Mohrman, D.E., Heller, L.J., 1997. Cardiovascular Physiology, 4th ed. McGraw-Hill, New York, pp. 47–69.

Nakayama, Y., Miyano, H., Shishido, T., Inagaki, M., Kawada, T., Sugimachi, M., Sunagawa, K., 2001. Heart rate-independent vagal effect on end-systolic elastance of the canine left ventricule under various levels of sympathetic tone. Circulation 104, 2277–2279.

Przyklenk, K., Kloner, R.A., 1995. Low-dose i.v. acetylcholine acts as a "preconditioning-mimetic" in the canine model. Journal of Cardiac Surgery 10, 389–395.

Rosenshtraukh, L., Danilo Jr., P., Anyukhovsky, E.P., Steinberg, S.F., Rybin, V., Brittain-Valenti, K., Molina-Viamonte, V., Rosen, M.R., 1994. Mechanisms for vagal modulation of ventricular repolarization and of coronary occlusion-induced lethal arrhythmias in cats. Circulation Research 75, 722–732.

Schömig, A., Fischer, S., Kurz, T., Richardt, G., Schömig, E., 1987. Nonexocytotic release of endogenous noradrenaline in the ischemic and anoxic rat heart: mechanism and metabolic requirements. Circulation Research 60, 194–205.

Schwartz, J.H., 2000. Neurotransmitters. In: Kandel, E.R., Schwartz, J.H., Jessell, T.M. (Eds.), Principles of Neural Science, 4th ed. McGraw-Hill, New York, pp. 280–297.

Snedecor, G.W., Cochran, W.G., 1989. Statistical Methods, 8th ed. Iowa State, Iowa, pp. 290–291.

Suga, H., Hisano, R., Goto, Y., Yamada, O., Igarashi, Y., 1983. Effect of positive inotropic agents on the relation between oxygen consumption and systolic pressure volume area in canine left ventricle. Circulation Research 53, 306–318.

Vanoli, E., De Ferrari, G.M., Stramba-Badiale, M., Hull Jr., S.S., Foreman, R.D., Schwartz, P.J., 1991. Vagal stimulation and prevention of sudden death in conscious dogs with a healed myocardial infarction. Circulation Research 68, 1471–1481.

Yamazaki, T., Akiyama, T., Kitagawa, H., Takauchi, Y., Kawada, T., Sunagawa, K., 1997. A new, concise dialysis approach to assessment of cardiac sympathetic nerve terminal abnormalities. American Journal of Physiology Heart and Circulatory Physiology 272, H1182–H1187.

Yamazaki, T., Akiyama, T., Mori, H., 2001. Effects of nociceptin on cardiac norepinephrine and acetylcholine release evoked by ouabain. Brain Research 904, 153–156.

Am J Physiol Heart Circ Physiol 291: H2187–H2191, 2006.
First published June 9, 2006; doi:10.1152/ajpheart.00175.2006.

Effects of Ca^{2+} channel antagonists on nerve stimulation-induced and ischemia-induced myocardial interstitial acetylcholine release in cats

Toru Kawada,[1] Toji Yamazaki,[2] Tsuyoshi Akiyama,[2] Kazunori Uemura,[1] Atsunori Kamiya,[1] Toshiaki Shishido,[1] Hidezo Mori,[2] and Masaru Sugimachi[1]

[1]Department of Cardiovascular Dynamics, Advanced Medical Engineering Center, National Cardiovascular Center Research Institute and [2]Department of Cardiac Physiology, National Cardiovascular Center Research Institute, Osaka, Japan

Submitted 17 February 2006; accepted in final form 7 June 2006

Kawada, Toru, Toji Yamazaki, Tsuyoshi Akiyama, Kazunori Uemura, Atsunori Kamiya, Toshiaki Shishido, Hidezo Mori, and Masaru Sugimachi. Effects of Ca^{2+} channel antagonists on nerve stimulation-induced and ischemia-induced myocardial interstitial acetylcholine release in cats. *Am J Physiol Heart Circ Physiol* 291: H2187–H2191, 2006. First published June 9, 2006; doi:10.1152/ajpheart.00175.2006.—Although an axoplasmic Ca^{2+} increase is associated with an exocytotic acetylcholine (ACh) release from the parasympathetic postganglionic nerve endings, the role of voltage-dependent Ca^{2+} channels in ACh release in the mammalian cardiac parasympathetic nerve is not clearly understood. Using a cardiac microdialysis technique, we examined the effects of Ca^{2+} channel antagonists on vagal nerve stimulation- and ischemia-induced myocardial interstitial ACh releases in anesthetized cats. The vagal stimulation-induced ACh release [22.4 nM (SD 10.6), $n = 7$] was significantly attenuated by local administration of an N-type Ca^{2+} channel antagonist ω-conotoxin GVIA [11.7 nM (SD 5.8), $n = 7$, $P = 0.0054$], or a P/Q-type Ca^{2+} channel antagonist ω-conotoxin MVIIC [3.8 nM (SD 2.3), $n = 6$, $P = 0.0002$] but not by local administration of an L-type Ca^{2+} channel antagonist verapamil [23.5 nM (SD 6.0), $n = 5$, $P = 0.758$]. The ischemia-induced myocardial interstitial ACh release [15.0 nM (SD 8.3), $n = 8$] was not attenuated by local administration of the L-, N-, or P/Q-type Ca^{2+} channel antagonists, by inhibition of Na^+/Ca^{2+} exchange, or by blockade of inositol 1,4,5-trisphosphate [Ins(1,4,5)P_3] receptor but was significantly suppressed by local administration of gadolinium [2.8 nM (SD 2.6), $n = 6$, $P = 0.0283$]. In conclusion, stimulation-induced ACh release from the cardiac postganglionic nerves depends on the N- and P/Q-type Ca^{2+} channels (with a dominance of P/Q-type) but probably not on the L-type Ca^{2+} channels in cats. In contrast, ischemia-induced ACh release depends on nonselective cation channels or cation-selective stretch activated channels but not on L-, N-, or P/Q type Ca^{2+} channels, Na^+/Ca^{2+} exchange, or Ins(1,4,5)P_3 receptor-mediated pathway.

cardiac microdialysis; ω-conotoxin GVIA; ω-conotoxin MVIIC; KB-R7943; verapamil; vagal stimulation

ALTHOUGH N-TYPE Ca^{2+} CHANNELS play a dominant role in norepinephrine release from sympathetic nerve endings (8, 33, 34), the type(s) of Ca^{2+} channels controlling ACh release in the mammalian parasympathetic system is not fully understood and show diversity among reports. To name a few, in isolated parasympathetic submandibular ganglia from the rat, neurotransmission is mediated by Ca^{2+} channels that are resistant to the L-, N-, P/Q-, and R- type Ca^{2+} channel antagonists (29). When the negative inotropic response to field stimulation was examined in the isolated guinea pig atria, Hong and Chang (8) reported the importance of P/Q-type Ca^{2+} channels, whereas Serone et al. (28) reported the importance of N-type Ca^{2+} channels. Because field stimulation in the isolated preparations could induce responses different from those in the in vivo conditions, we aimed to examine the effects of Ca^{2+} channel antagonists on the vagal nerve stimulation-induced myocardial interstitial ACh release in the in vivo feline heart.

Aside from the important role of the normal physiological regulation of the heart, the vagal nerve can be a therapeutic target for certain cardiovascular diseases (2, 3, 13, 22, 27). In previous studies, we have shown that acute myocardial ischemia causes myocardial interstitial ACh release in the ischemic region independently of efferent vagal nerve activity (12, 14). The comparison of the effects of Ca^{2+} channel antagonists on the ACh releases induced by vagal nerve stimulation and by acute myocardial ischemia may deepen our understanding about the ischemia-induced myocardial interstitial ACh release.

A cardiac microdialysis technique offers detailed analyses of in vivo myocardial interstitial ACh release (1, 15). Because the local administration of pharmacological agents through a dialysis probe can modulate ACh release without significantly affecting systemic hemodynamics, a combination of cardiac microdialysis with local pharmacological interventions is useful for analyzing the mechanisms of ACh release in vivo. In the present study, we examined the effects of Ca^{2+} channel antagonists on nerve stimulation- and ischemia-induced ACh releases in anesthetized cats. The results indicate that stimulation-induced ACh release from the cardiac parasympathetic postganglionic nerves depends on the N- and P/Q-type Ca^{2+} channels but probably not on the L-type Ca^{2+} channels. In contrast, ischemia-induced myocardial interstitial ACh release is resistant to the inhibition of L-, N-, and P/Q-type Ca^{2+} channels. In addition, the ischemia-induced myocardial ACh release is resistant to the inhibition of Na^+/Ca^{2+} exchanger and the blockade of inositol 1,4,5-trisphosphate [Ins(1,4,5)P_3] receptor but is suppressed by gadolinium, suggesting that nonselective cation channels or cation-selective stretch-activated channels are involved.

MATERIALS AND METHODS

Common Preparation

Animal care was provided in accordance with the *Guiding Principles for the Care and Use of Animals in the Field of Physiological*

Address for reprint requests and other correspondence: T. Kawada, Dept. of Cardiovascular Dynamics, Advanced Medical Engineering Center, National Cardiovascular Center Research Institute, 5-7-1 Fujishirodai, Suita, Osaka 565-8565, Japan (e-mail: torukawa@res.ncvc.go.jp).

The costs of publication of this article were defrayed in part by the payment of page charges. The article must therefore be hereby marked "*advertisement*" in accordance with 18 U.S.C. Section 1734 solely to indicate this fact.

Sciences approved by the Physiological Society of Japan. All protocols were approved by the Animal Subjects Committee of the National Cardiovascular Center. Adult cats weighing from 2.2 to 4.2 kg were anesthetized via an intraperitoneal injection of pentobarbital sodium (30–35 mg/kg) and ventilated mechanically with room air mixed with oxygen. The depth of anesthesia was maintained with a continuous intravenous infusion of pentobarbital sodium (1–2 $mg \cdot kg^{-1} \cdot h^{-1}$) through a catheter inserted from the right femoral vein. Systemic arterial pressure was monitored from a catheter inserted from the right femoral artery. The vagi were sectioned bilaterally at the neck. The esophageal temperature of the animal, which was measured by a thermometer (CTM-303, TERUMO, Japan), was maintained at around 37°C using a heated pad and a lamp.

With the animal in the lateral position, the left fifth and sixth ribs were resected to expose the heart. A dialysis probe was implanted transversely, using a fine guiding needle, into the anterolateral free wall of the left ventricle perfused by the left anterior descending coronary artery (LAD). Heparin sodium (100 U/kg) was administered intravenously to prevent blood coagulation. At the end of the experiment, the experimental animals were killed with an overdose of pentobarbital sodium. Postmortem examination confirmed that the dialysis probe had been threaded in the middle layer of the left ventricular myocardium. The thickness of the left ventricular free wall was ~7–8 mm, and the semipermeable membrane of the dialysis probe was positioned ~3–4 mm from the epicardial surface.

Dialysis Technique

The materials and properties of the dialysis probe have been described previously (1). Briefly, we designed a transverse dialysis probe. A dialysis fiber of semipermeable membrane (13 mm length, 310 μm OD, 200 μm ID; PAN-1200, 50,000 molecular weight cutoff, Asahi Chemical, Japan) was glued at both ends to polyethylene tubes (25 cm length, 500 μm OD, 200 μm ID). The dialysis probe was perfused at a rate of 2 μl/min with Ringer solution containing a cholinesterase inhibitor eserine (physostigmine, 100 μM). Experimental protocols were started 2 h after the dialysis probe was implanted when the ACh concentration in the dialysate reached a steady state. The ACh concentration in the dialysate was measured by high-performance liquid chromatography with electrochemical detection (Eicom, Kyoto, Japan).

Local administration of a pharmacological agent was carried out through a dialysis probe. That is to say, we added the pharmacological agent to the perfusate and allowed 1 h for a settling time. The pharmacological agent should spread around the semipermeable membrane, thereby affecting the neurotransmitter release in the vicinity of the semipermeable membrane. Because the distribution across the semipermeable membrane is required, based on previous results (33, 34), we used the pharmacological agent at the concentration 10–100 times higher than that required for complete channel blockade in experimental settings in vitro.

Specific Preparation and Protocols

Protocol 1. Bipolar platinum electrodes were attached bilaterally to the cardiac ends of the sectioned vagi at the neck. The nerves and electrodes were covered with warmed mineral oil for insulation. The vagal nerves were stimulated for 15 min (20 Hz, 1 ms, 10 V). We measured the stimulation-induced ACh release in the absence of Ca^{2+} channel blockade (control, $n = 7$) and examined the effects of an L-type Ca^{2+} channel antagonist verapamil (100 μM, $n = 5$), an N-type Ca^{2+} channel antagonist ω-conotoxin GVIA (10 μM, $n = 7$), a P/Q-type Ca^{2+} channel antagonist ω-conotoxin MVIIC (10 μM, $n = 6$), and combined administration of ω-conotoxin GVIA and ω-conotoxin MVIIC (10 μM each, $n = 6$).

Protocol 2. Because a preliminary result from *protocol 1* suggested that local administration of verapamil was ineffective in suppressing stimulation-induced ACh release, we examined the effects of the intravenous administration of verapamil (300 μg/kg, $n = 6$) on stimulation-induced ACh release in vagotomized animals as a supplemental experiment.

Protocol 3. A 60-min LAD occlusion was performed by using a 3-0 silk suture passed around the LAD just distal to the first diagonal branch. We measured the ACh levels during 45–60 min of ischemia in the absence of Ca^{2+} channel blockade (control, $n = 8$) and examined the effects of verapamil (100 μM, $n = 5$), ω-conotoxin GVIA (10 μM, $n = 5$), and ω-conotoxin MVIIC (10 μM, $n = 5$). A previous result indicated that the ischemia-induced ACh release reached the steady state during 45–60 min of ischemia (14). We also examined the effects of three additional agents, a Na^+/Ca^{2+} exchange inhibitor KB-R7943 (10 μM, $n = 5$) (9, 10), an Ins(1,4,5)P_3 receptor blocker xestospongin C (500 μM, $n = 6$) (25), and a nonselective cation channel blocker or a cation-selective stretch activated channel blocker gadolinium (1 mM) (5, 17), on the ischemia-induced ACh release.

Statistical Analysis

All data are presented as mean (SD) values. In *protocol 1*, we compared stimulation-induced ACh release among the five groups using one-way analysis of variance followed by the Student-Neuman-Keuls test (6). In *protocol 2*, we used an unpaired-*t* test (two-sided) to examine the effect of intravenous verapamil administration on stimulation-induced ACh release. In *protocol 3*, we compared ischemia-induced ACh release among the seven groups using one-way analysis of variance followed by the Dunnett' test against the control. For all analyses, differences were considered significant when $P < 0.05$.

RESULTS

In *protocol 1*, the ACh level during electrical vagal stimulation was 22.4 nM (SD 10.6). Local administration of verapamil did not affect stimulation-induced ACh release (Fig. 1). In contrast, local administration of ω-conotoxin GVIA or ω-conotoxin MVIIC suppressed stimulation-induced ACh release. The extent of suppression was greater in the latter. The ACh level was significantly lower in the simultaneous administration group (ω-conotoxin GVIA + ω-conotoxin MVIIC)

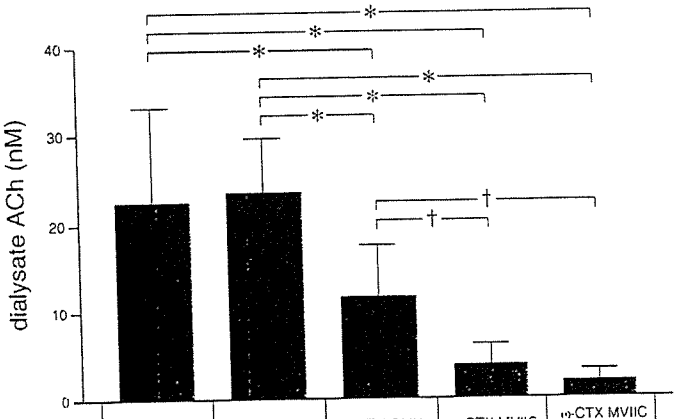

	vehicle	verapamil	ω-CTX GVIA	ω-CTX MVIIC	ω-CTX MVIIC + ω-CTX GVIA
vehicle		0.758	0.0054	0.0002	0.0002
verapamil	0.758		0.0068	0.0002	0.0001
GVIA	0.0054	0.0068		0.033	0.025
MVIIC	0.0002	0.0002	0.033		0.581
MVIIC+GVIA	0.0002	0.0001	0.025	0.581	

Fig. 1. Effects of local administration of verapamil, ω-conotoxin GVIA, ω-conotoxin MVIIC, or ω-conotoxin GVIA plus ω-conotoxin MVIIC on vagal nerve stimulation-induced myocardial interstitial ACh release. Both ω-conotoxin GVIA and ω-conotoxin MVIIC, but not verapamil, suppressed stimulation-induced ACh release. Data are mean (SD) values. *$P < 0.01$, †$P < 0.05$. The exact P values are presented.

than that in the ω-conotoxin GVIA group but was not different from the ω-conotoxin MVIIC group.

In *protocol 2*, the intravenous administration of verapamil did not significantly change stimulation-induced ACh release [21.7 nM (SD 12.8)] compared with the control group ($P = 0.91$).

In *protocol 3*, the ACh level in the ischemic region was 14.9 nM (SD 8.3) during 45–60 min of acute myocardial ischemia. Inhibition of voltage-dependent Ca^{2+} channels by local administration of verapamil, ω-conotoxin GVIA, or ω-conotoxin MVIIC did not affect ischemia-induced ACh release (Fig. 2). Inhibition of the reverse mode action of Na^+/Ca^{2+} exchange by local administration of KB-R7943 appeared to have augmented rather than suppressed ischemia-induced ACh release, though there was no statistically significant difference from the control. Blockade of the Ins(1,4,5)P_3 receptor by local administration of xestospongin C did not affect the ischemia-induced ACh release. In contrast, blockade of nonselective cation channels or cation-selective stretch-activated channels by local administration of gadolinium suppressed the ischemia-induced ACh release.

DISCUSSION

Ca^{2+} Channels Involved in Stimulation-Induced ACh Release

Although neurotransmitter release at mammalian sympathetic neuroeffector junctions predominantly depends on Ca^{2+} influx through N-type Ca^{2+} channels (23, 33, 34), the type(s) of Ca^{2+} channels involved in ACh release from cardiac parasympathetic neuroeffector junctions show diversity among reports (8, 28). One possible factor hampering investigations into parasympathetic postganglionic neurotransmitter release in response to vagal nerve stimulation in vivo is that the parasympathetic ganglia are usually situated in the vicinity of the effector organs, thereby making it difficult to separately assess ACh release from preganglionic and postganglionic nerves. In the previous study from our laboratory, intravenous administration, but not local administration of a ganglionic blocker, hexamethonium reduced vagal stimulation-induced ACh release assessed by cardiac microdialysis (1). The negligible effect of local hexamethonium administration on stimulation-induced ACh release suggests the lack of parasympathetic ganglia around the dialysis probe. In support of our speculation, a recent neuroanatomical finding indicates that three ganglia, away from the left anterior free wall targeted by the dialysis probe, provide the major source for left ventricular postganglionic innervation in cats: a cranioventricular ganglion, a left ventricular ganglion 2 (so designated), and an interventriculo-septal ganglion (11). Therefore, ACh, as measured by cardiac microdialysis, is considered to predominantly reflect ACh release from parasympathetic postganglionic nerves.

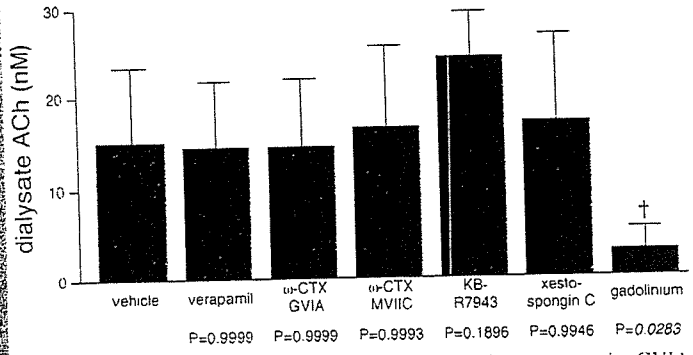

Fig. 2. Effects of local administration of verapamil, ω-conotoxin GVIA, ω-conotoxin MVIIC, KB-R7943, xestospongin C, or gadolinium on acute myocardial ischemia-induced myocardial interstitial ACh release in the ischemic region. Gadolinium alone suppressed the ischemia-induced ACh release. Data are mean (SD) values. †$P < 0.05$. The exact P values are presented.

Local (*protocol 1*) or intravenous (*protocol 2*) administration of verapamil did not affect stimulation-induced ACh release. In contrast, vagal stimulation-induced ACh release was reduced in both the ω-conotoxin GVIA and ω-conotoxin MVIIC groups but to a greater extent in the latter (Fig. 1). Therefore, both N- and P/Q-type, but probably not L-type, Ca^{2+} channels are involved in stimulation-induced ACh release from the cardiac parasympathetic postganglionic nerves in cats. The contribution of P/Q type Ca^{2+} channels to ACh release might be greater than that of N-type Ca^{2+} channels. Hong and Chang (8) reported that the negative inotropic response to field stimulation depends predominantly on the P/Q-type Ca^{2+} channels in isolated guinea pig atria, whereas Serone et al. (28) reported the predominance of N-type Ca^{2+} channels. In those studies, the field stimulation employed differed from ordinary activation of the postganglionic nerves by nerve discharge and, in addition, ACh release was not directly measured. The present study directly demonstrated the involvement of P/Q- and N-type Ca^{2+} channels in the stimulation-induced ACh release in the cardiac parasympathetic postganglionic nerves. These results support the concept that multiple subtypes of the voltage-gated Ca^{2+} channel mediate transmitter release from the same population of parasympathetic neurons (31).

Stimulation-induced ACh release was suppressed by ~50% in the ω-conotoxin GVIA group and by ~80% in the ω-conotoxin MVIIC group. The algebraic summation of the extent of suppression exceeded 100%. The phenomenon may be in part due to the nonlinear dose-response relationship between Ca^{2+} influx and transmitter release (32). The supra-additive phenomenon may be also due to the affinity of ω-conotoxin MVIIC to N-type Ca^{2+} channels (8, 26, 36). Combined local administration of ω-conotoxin GVIA and ω-conotoxin MVIIC almost completely suppressed stimulation-induced ACh release to a level similar to that achieved by the Na^+ channel inhibitor tetrodotoxin (15). Therefore, involvement of another untested type of Ca^{2+} channel(s) is unlikely in the stimulation-induced ACh release from the cardiac parasympathetic postganglionic nerves in cats.

Ca^{2+} Channels and Ischemia-Induced ACh Release

In a previous study, we showed that acute myocardial ischemia evokes myocardial interstitial ACh release in the ischemic region via a local mechanism independent of efferent vagal nerve activity (14). In that study, the inhibition of intracellular Ca^{2+} mobilization by local administration of 3,4,5-trimethoxybenzoic acid 8-(diethyl amino)-octyl ester (TMB-8) suppressed ischemia-induced ACh release, suggesting that an axoplasmic Ca^{2+} elevation is essential for the ischemia-induced ACh release. Because tissue K^+ concentration increases in the ischemic region (7, 18), high K^+-induced

depolarization could activate voltage-dependent Ca^{2+} channels even in the absence of efferent vagal nerve activity. However, ischemia-induced ACh release was not suppressed by local administration of verapamil, ω-conotoxin GVIA, or ω-conotoxin MVIIC (Fig. 2). Therefore, Ca^{2+} entry through the voltage-dependent Ca^{2+} channels is unlikely a mechanism for the ischemia-induced myocardial interstitial ACh release.

Acute myocardial ischemia causes energy depletion in the ischemic region, which impairs Na^+-K^+-ATPase activity. Ischemia also causes acidosis in the ischemic region, which promotes Na^+/H^+ exchange. As a result, ischemia causes intracellular Na^+ accumulation. The decrease in the Na^+ gradient across the plasma membrane may then cause the Na^+/Ca^{2+} exchanger to operate in the reverse mode, facilitating intracellular Ca^{2+} overload. KB-R7943 can inhibit the reverse mode of Na^+/Ca^{2+} exchange (9, 10) and its potential to protect against ischemia-reperfusion injury has been reported (21). In the present study, however, local administration of KB-R7943 failed to suppress and rather increased ACh release during ischemia as opposed to our expectation. It is plausible that the inhibition of reverse mode of Na^+/Ca^{2+} may have facilitated the accumulation of intracellular Na^+ and induced adverse effects that cancelled the possible beneficial effects derived from the inhibition of Ca^{2+} entry through the Na^+/Ca^{2+} exchanger itself. In addition, KB-R7943 could inhibit the forward mode of Na^+/Ca^{2+} exchange and reduce Ca^{2+} efflux (16), contributing to the intracellular Ca^{2+} accumulation and ACh release. In the present study, we observed the effects of KB-R7943 only during the ischemic period. However, accumulation of intracellular Na^+ through Na^+/H^+ exchange is enhanced on reperfusion due to the washout of extracellular H^+ (20). The inhibition of Na^+/Ca^{2+} exchange to suppress Ca^{2+} overload might become more important during the reperfusion phase. For instance, the percent segment shortening of the left ventricle was improved by KB-R7943 during reperfusion but not during ischemia (35).

As already mentioned, the ischemia-induced ACh release can be blocked by TMB-8 and thus the intracellular Ca^{2+} mobilization is required for the ischemia-induced ACh release (14). Besides the Ca^{2+} entries through voltage-dependent Ca^{2+} channels and via the reverse mode of Na^+/Ca^{2+} exchanger, Ca^{2+} may be mobilized from the endoplasmic reticulum via pathological pathways. As an example, the mitochondrial permeability transition pore triggered in pathological conditions is linked to cytochrome *c* release. Cytochrome *c* can bind to the endoplasmic reticulum Ins(1,4,5)P_3 receptor, rendering the channel insensitive to autoinhibition by high cytosolic Ca^{2+} concentration and resulting in enhanced endoplasmic reticulum Ca^{2+} release (4, 30). In the present study, however, blockade of Ins(1,4,5)P_3 receptor by xestospongin C failed to suppress the ischemia-induced ACh release. In contrast, local administration of gadolinium significantly suppressed the ischemia-induced ACh release. Therefore, nonselective cation channels or cation-selective stretch-activated channels contribute to the ischemia-induced ACh release. During myocardial ischemia, the ischemic region can be subjected to paradoxical systolic bulging. Such bulging likely opens stretch-activated channels and causes myocardial interstitial ACh release, possibly leading to cardioprotection by ACh against ischemic injury (2).

Limitations

First, the experiment was performed under anesthetic conditions, which may have influenced basal autonomic activity. However, because we sectioned the vagi at the neck, basal autonomic activity may have had only a minor effect on ACh release during the vagal stimulation and during acute myocardial ischemia. Second, we added eserine to the perfusate to inhibit immediate degradation of ACh (24), which may have increased the ACh level in the synaptic cleft and activated regulatory pathways such as autoinhibition of ACh release via muscarinic receptors (24). However, the myocardial interstitial ACh level measured under this condition could reflect changes induced by Na^+ channel inhibitor, choline uptake inhibitor, and vesicular ACh transport inhibitor as described in a previous study (15). Therefore, we think that the interpretation of the present results is reasonable. Third, tissue and species differences should be taken into account when extrapolating the present findings, because significant heterogeneity in the Ca^{2+} channels involved in the mammalian parasympathetic system may exist. Finally, we used verapamil to test the involvement of L-type Ca^{2+} channels in the ACh release. There are three major types of L-type Ca^{2+} channel antagonists with different binding domains (verapamil, nifedipine, and diltiazem) (19). Whether the effects on the ACh release are common among the three types of L-type Ca^{2+} channel antagonists remains unanswered.

In conclusion, the N- and P/Q-type Ca^{2+} channels (with the P/Q-type dominant), but probably not the L-type Ca^{2+} channels, are involved in vagal stimulation-induced ACh release from the cardiac parasympathetic postganglionic nerves in cats. In contrast, myocardial interstitial ACh release in the ischemic myocardium is resistant to the blockade of L-, N-, and P/Q-type Ca^{2+} channels. In addition, the ischemia-induced myocardial ACh release is resistant to the inhibition of Na^+/Ca^{2+} exchanger and the blockade of Ins(1,4,5)P_3 receptor but is suppressed by gadolinium, suggesting that nonselective cation channels or cation-selective stretch-activated channels are involved.

GRANTS

This study was supported by Health and Labour Sciences Research Grant for Research on Advanced Medical Technology from the Ministry of Health, Labour and Welfare of Japan, Health and Labour Sciences Research Grant for Research on Medical Devices for Analyzing, Supporting and Substituting the Function of Human Body from the Ministry of Health, Labour and Welfare of Japan, Health and Labour Sciences Research Grant H18-Iryo-Ippan-023 from the Ministry of Health, Labour and Welfare of Japan, Program for Promotion of Fundamental Studies in Health Science from the National Institute of Biomedical Innovation, a Grant provided by the Ichiro Kanehara Foundation, Ground-based Research Announcement for Space Utilization promoted by Japan Space Forum, and Industrial Technology Research Grant Program in 03A47075 from New Energy and Industrial Technology Development Organization of Japan.

REFERENCES

1. **Akiyama T, Yamazaki T, and Ninomiya I.** In vivo detection of endogenous acetylcholine release in cat ventricles. *Am J Physiol Heart Circ Physiol* 266: H854–H860, 1994.
2. **Ando M, Katare RG, Kakinuma Y, Zhang D, Yamasaki F, Muramoto K, and Sato T.** Efferent vagal nerve stimulation protects heart against ischemia-induced arrhythmias by preserving connexin43 protein. *Circulation* 112: 164–170, 2005.